

# **PLASTIC WASTES TO ENERGY: PYROLYSIS SIMULATION BY THERMOGRAVIMETRY**

**Faith Eferemo Okoro**

Thesis to obtain the Master of Science Degree in

## **Energy Engineering and Management**

Supervisors: Prof. Ana Paula Vieira Soares Pereira Dias

Dr. Ana Filipa da Silva Ferreira

### **Examination Committee**

Chairperson: Prof. Francisco Manuel Da Silva Lemos

Supervisor: Prof. Ana Paula Vieira Soares Pereira Dias

Member of the Committee: Prof. Jaime Filipe Borges Puna

**November 2019**

## Special acknowledgement

This thesis is based on the work conducted within the Innoenergy Master School, in the MSc program Clean Fossil and Alternative Fuels Energy. This program is supported financially by the Innoenergy. This author also received financial support from Innoenergy, which is gratefully acknowledged.

*Innoenergy is a company supported by the European Institute of Innovation and Technology (EIT) and has the mission of delivering commercial products and services, new businesses, innovators and entrepreneurs in the field of sustainable energy through the integration of higher education, research, entrepreneurs and business companies. Shareholders in Innoenergy are leading industries, research centers, universities and business schools from across Europe.*

[www.innoenergy.com](http://www.innoenergy.com)



**MSc Clean Fossil and Alternative Fuels Energy is a collaboration of:**

**AGH University of Science and Technology, Krakow, Poland**

**SUT Silesian University of Technology, Katowice, Poland**

**IST Institute Superior Tecnico, Lisbon, Portugal**

(The MSc thesis was prepared at IST Institute Superior Tecnico, Lisbon, Portugal)



## Acknowledgements

I am pleased to acknowledge the tremendous support and encouragement of all who, in different ways contributed to the successful completion and execution of this thesis. My sincere gratitude goes to my supervisor, Prof. Ana Paula Vieira Soares Pereira Dias for her time, patience and support. Her impeccable supervision, modeled this thesis to be the best.

Special thanks goes to my parents, who believed in me against all odds, prayed for me and supported me throughout the whole process. To my siblings' thanks for all the tender love and care.

Special thanks goes to my yummy buddy, Olapade Olushola Tomilayo for his tiredless effort in going through my results, fixing the bugs in MathLab during the simulation process, his positivity was amazing, he believed in me when I could not even believe myself. Thanks Jejun!

I would also like to thank Marta, whose husband provided the reference plastic that was used in comparison with waste plastics. Also thanks to Monica who helped me with the Fourier Transform Analysis of waste plastics.

To my friends, thanks for always remembering to keep plastics for me, proof reading my theis and the constructive criticism even though it hurt sometimes, made this thesis great. You all are the best.

## Abstract

The world is finally waking up to the plastic problem which is like a ticking time bomb set to explode with the increasing amount of plastic waste that is been generated daily. This research work studied the thermal degradation of plastic waste and kinetic modelling process which can be useful in the determination of key operating design and parameters.

Kinetic modelling requires significant amount of information about kinetic parameters, especially the activation energy. Thermogravimetric analysis (TGA) was used to obtain kinetic data with degradation taking place in a single step process. The kinetic analysis was studied by conventional thermogravimetric technique (Direct Arrhenius Method, Coat & Redfern and Horowitz and Metzger) with single heating rate(30°C/min) in nitrogen atmosphere for the different plastic waste. The activation energy obtained using the different approach for the plastic ABS\_White, ABS\_Blue, ABS (30) PS, LDPE, NYLON and PET was (219, 240, 188, 222, 260, 175, 304), (226, 189, 224, 382,275,186, 347) kJ/mol respectively. The result obtained using these models were in accordance with published data however these models use unrealistic assumptions that may not be accurate in predicting the true degradation behavior of the polymer, hence it cannot give a proper understanding of how pyrolysis occur and how the process can be optimized thus the reason for the distributed activation energy analysis model (DAEM)

The DAEM algorithm was developed using MATLAB with data obtained from TGA experiments which was used in calculation of kinetic parameters. The results obtained from the simulation were able to effectively model the degradation behavior of the different plastics in this study, thus, predicted the thermal behavior of plastics at different heating rates.

Keywords: Plastic wastes, Pyrolysis Kinetics, Thermogravimetry, Distributed Activation Energy Model.

## Resumo

Finalmente, o mundo está acordando para o problema do plástico, que é como uma bomba-relógio que explode com a crescente quantidade de lixo plástico que é gerado diariamente. Este trabalho de pesquisa estudou a degradação térmica dos resíduos de plástico e o processo de modelagem cinética, que pode ser útil na determinação dos principais parâmetros e projeto operacional.

A modelagem cinética requer uma quantidade significativa de informações sobre parâmetros cinéticos, especialmente a energia de ativação. A análise termogravimétrica (TGA) foi usada para obter dados cinéticos com a degradação ocorrendo em um processo de etapa única. A análise cinética foi estudada pela técnica termogravimétrica convencional (método direto de Arrhenius, Coat & Redfern e Horowitz e Metzger) com taxa de aquecimento único (30°C / min) em atmosfera de nitrogênio para os diferentes resíduos plásticos. A energia de ativação obtida usando a abordagem diferente para o plástico ABS\_Branco, ABS\_Blue, ABS (30) PS, LDPE, NYLON e PET foi (219, 240, 188, 222, 260, 175, 304), (226, 189, 224, 382, 275, 186, 347) kJ / mol, respectivamente. O resultado obtido com esses modelos estava de acordo com os estudos de literatura, mas esses modelos usam premissas irreais que podem não ser precisas na previsão do verdadeiro comportamento de degradação do polímero, portanto, não podem fornecer um entendimento adequado de como ocorre a pirólise e como o processo pode ser realizado. otimizado, portanto, o motivo do modelo de análise de energia de ativação distribuída (DAEM)

O algoritmo DAEM foi desenvolvido usando o MATLAB com dados obtidos de experimentos TGA que foram utilizados no cálculo de parâmetros cinéticos. Os resultados obtidos na simulação foram capazes de modelar efetivamente o comportamento de degradação dos diferentes plásticos deste estudo, prevendo, assim, o comportamento térmico dos plásticos em diferentes taxas de aquecimento.

Palavras-Chaves: Resíduos plásticos, cinética de pirólise, termogravimetria, modelo de energia de ativação distribuída.

# Table of Contents

Special acknowledgement .....	ii
Acknowledgements .....	iii
Abstract .....	iv
Resumo .....	v
List of Tables .....	viii
List of Figures .....	ix
List of Abbreviations .....	x
1. Introduction .....	1
1.1 The Plastic Problem .....	1
1.1.1 Plastic Consumption and Production .....	1
1.1.2 Plastic Waste Impact .....	2
1.1.2.1 Impact on Environment .....	3
1.1.2.2 Impacts on Animals .....	3
1.1.2.3 Impacts on Humans .....	4
1.2 Plastic Waste Management .....	4
1.3 Plastic Waste to Energy .....	5
1.4 Objectives .....	6
2 Thermal degradation of plastic waste .....	7
2.1 Polymer .....	7
2.2 Chemical Composition of Plastics .....	8
2.3 Degradation Reaction Mechanism .....	9
2.4 Pyrolysis Reaction Stages .....	11
2.5 Development of Kinetic Models .....	14
2.5.1 Thermogravimetric Curve .....	15
2.5.2 Factors Influencing Thermogravimetry Analysis .....	16
2.5.3 Kinetics Analysis of Thermogravimetric Data .....	16
3 Materials and Methods .....	24
3.1 Materials .....	24
3.1.1 Plastics .....	24
3.2 Plastic Characterization .....	24
3.2.1 Fourier Transform Infrared Spectroscopy (FTIR) .....	24
3.2.1 Thermogravimetric Analysis (TGA) .....	27
3.2.1.1 Determination of Kinetic Parameters .....	28
3.3 Kinetics Modelling .....	29
3.3.1 Development of Kinetic Model .....	29

4	Results and Discussion .....	33
4.1	Plastic Characterization.....	33
4.1.1	Fourier Transform Infrared Spectroscopy (FTIR).....	33
4.1.2	Thermogravimetry Analysis .....	36
4.2	Determination of Kinetic Parameters .....	38
4.2.1	Graphical Method.....	38
4.2.2	Horowitz and Metzger.....	40
4.2.3	Comparison of Kinetic Parameters.....	41
4.3	Distributed Activation Energy Model .....	45
4.3.1	Comparison of Experimental Result with Simulated Result .....	45
4.3.2	Determination of Kinetic Parameters .....	47
4.3.3	Predicting Thermal Behavior of Plastics .....	50
5.	Conclusions and Future Works.....	51
	Bibliography .....	53
	Annex .....	59

## List of Tables

Table 1-1: Comparison of energy density of plastics and different types of fuels (Baines, 1993).....	5
Table 2-1: Proximate Analysis of Plastics (Abnisa F, 2014) .....	8
Table 3-1: Functional Groups and Component Classes in the FTIR Spectrum for Polymer Material ..	25
Table 4-1: Grouped Municipal Solid Plastic Waste.....	35
Table 4-2: Kinetic Parameters Obtained by Direct Arrhenius Model .....	39
Table 4-3: Parameters Obtained by Coat & Redfern Model.....	40
Table 4-4: Kinetic Parameters Obtained by Horowitz And Metzger Model .....	41
Table 4-5: Comparison of Activation energies .....	44
Table 4-6: Kinetic Parameters obtained with DAEM for ABS .....	48
Table 4-7: Kinetic Parameters obtained with DAEM for PS, LDPE, PET and NYLON.....	49
Table A-1: Summary of Temperature Ranges for Different Polymer Material.....	59



## List of Figures

Figure 1-1: Plastic Waste Generated by Polymer Type (Geyer, 2017) .....	1
Figure 1-2: Global Plastics Production (Geyer, 2017) .....	2
Figure 1-3: Plastic Consumption by Different Sectors (Geyer, 2017).....	2
Figure 1-4 Surface plastic mass by ocean basin, 2013 (Eriksen, 2014) .....	3
Figure 1-5 Plastic pollution in our world seas', and its effect on animals and humans (Arthur, 2017) ...	4
Figure 1-6 Global Plastic Waste by disposal (Geyer, 2017) .....	5
Figure 2-1 Polymer structures. (Dutton, 2018).....	7
Figure 2-2 The phase transitions of PET by differential thermal analysis. (Wunderlich, 2005) .....	9
Figure 2-3 Effect of temperature on elastic modulus of polymers (Wade, 1995) .....	10
Figure 2-4 Stability of carbon bonds (Wade, 1995) .....	10
Figure 2-5 Radical mechanism of the thermal degradation of polypropylene (H. Bockhorn, 1999) .....	12
Figure 2-6 Reaction rate as a function of Temperature and heating rate in PET Pyrolysis (Saha, 2005) .....	13
Figure 2-7 Influence of Pressure on the Distribution of Product from PE Pyrolysis (Murata, 2004).....	14
Figure 2-8 Non-Isothermal Thermogravimetric analysis of plastics (Richardson, 2012) .....	15
Figure 3-1 Plastic Waste .....	24
Figure 3-2 Perkin-Elmer Spectrum Two FT-IR Spectrometer.....	26
Figure 3-3 TG-DTA/DSC Sateram labsys.....	27
Figure 3-4 Work Flow of Experimental and Modelling Process .....	32
Figure 4-1 FTIR Spectra of PET .....	33
Figure 4-2 FTIR Spectra of HDPE .....	33
Figure 4-3 FTIR Spectra of LDPE.....	33
Figure 4-4 FTIR Spectra of PP.....	34
Figure 4-5 FTIR Spectra of PS.....	34
Figure 4-6 FTIR Spectra of ABS .....	35
Figure 4-7 FTIR Spectra of NYLON.....	35
Figure 4-8 Thermogravimetric Analysis (TGA) of Plastic Waste .....	36
Figure 4-9 Derivative thermogravimetry (DTG) of Plastic Waste.....	37
Figure 4-10 Kinetics Models Plots for ABS_White.....	42
Figure 4-11 Kinetic Models Plots for ABS_Blue.....	42
Figure 4-12 Kinetic Models Plots for ABS (30) .....	42
Figure 4-13 Kinetic Models Plots for LDPE.....	43
Figure 4-14 Kinetic Models Plots for NYLON.....	43
Figure 4-15 Kinetic Models Plots for PS .....	43
Figure 4-16 Kinetic Models Plots for PET .....	44
Figure 4-17 Gaussian distribution curves fitted on DTG Experimental results .....	47
Figure 4-18 Activation Energy Distribution.....	47
Figure 4-19 Relationship between activation energy and conversion( $V/V^*$ ).....	48
Figure 4-20 DTG prediction at different heating rate .....	50

## List of Abbreviations

<b>A</b>	Pre-exponential factor or frequency factor [ $\text{min}^{-1}$ ]
<b>ABS</b>	Acrylonitrile butadiene styrene
<b><math>\alpha</math></b>	Degree/extent of conversion
<b><math>\beta</math></b>	heating rate, $dT/dt$ [ $^{\circ}\text{C min}^{-1}$ ]
<b>CR</b>	Coat & Redfern
<b>DA</b>	Direct Arrhenius
<b>DAEM</b>	Distributed Activation Energy Model
<b>DTG curve</b>	First derivative of the mass loss curve obtained from the Thermogravimetric Analyzer
<b><math>d\alpha/dt</math></b>	Conversion rate, as function of time [ $\text{min}^{-1}$ ]
<b><math>d\alpha/dT</math></b>	Conversion rate, as function of temperature
<b>E</b>	Activation energy [ $\text{kJ/mol}$ ]
<b>E0</b>	Mean value of the activation energy when using the DAEM [ $\text{kJ/mol}$ ];
<b><math>f(\alpha)</math></b>	Conversion function dependent on the reaction mechanism
<b><math>f(E)</math></b>	Distribution function of the activation energy when using the DAEM
<b>HDPE</b>	High-density polyethylene
<b>LDPE</b>	Low-density polyethylene
<b>n</b>	Order of reaction
<b>PE</b>	Polyethylene
<b>PET</b>	Polyethylene terephthalate
<b>PP</b>	Polypropylene
<b>PS</b>	Polystyrene
<b>PVC</b>	Polyvinyl chloride
<b>TGA</b>	Thermogravimetric Analysis

# 1. Introduction

## 1.1 The Plastic Problem

Society throw-away culture, which is strongly influenced by consumerism, is steadily increasing the amount of waste generated. The amount and type of waste generated is determined by rate of urbanization, level of economic development and population growth. According to (WorldBank, 2019), the world generates 2.01 billion tonnes of Municipal Solid Waste which corresponds to the waste generate per person per day ranging from 0.11 – 4.54kilograms. Annual waste generated is expected to increase by 70% to about 3.4 billion tonnes in 2050 due to rapid increase in population and urbanization.

Plastics contribute to approximately 10% of discarded waste (Geyer, 2017) and only about 25% is being recycled (Fig 1-1). Plastic wastes are non-homogeneous group of materials that differ not only with regards to their chemical composition or previous application field, but also quality, (purity or contamination level). Plastics key strengths are its durability, versatility however, these strengths have become its greatest weakness which is its non-degradability. This is the plastic paradox.

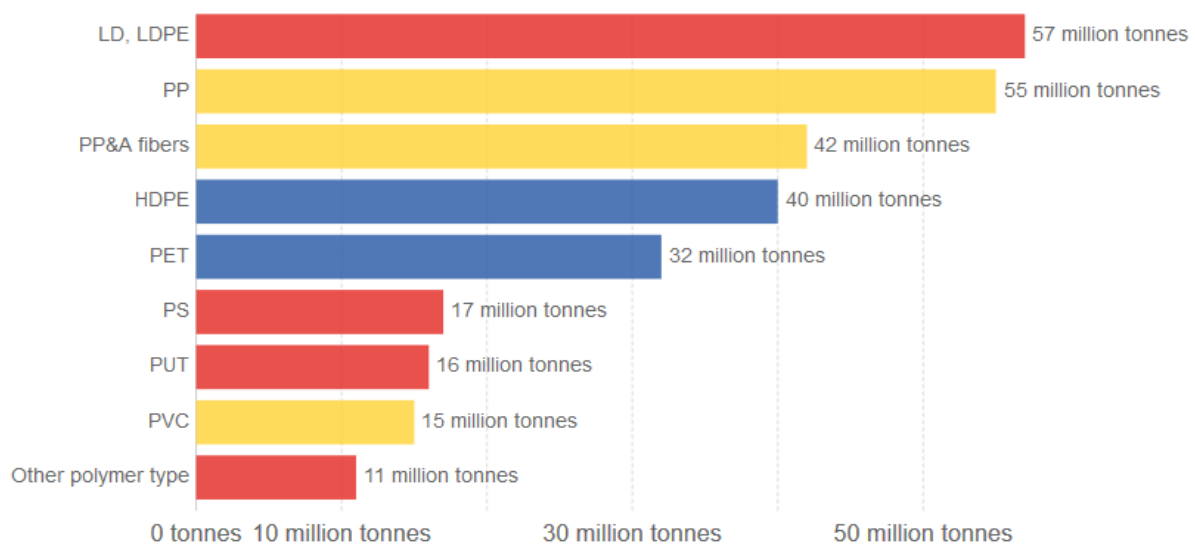


Figure 1-1: Plastic Waste Generated by Polymer Type<sup>1</sup> (Geyer, 2017)

### 1.1.1 Plastic Consumption and Production

From Fig. 1.2, it can be observed that the plastic production has increased since 1950 which was initially 2 million tonnes/year. Cumulatively, as at 2015, the world has produced 7.8 billion tonnes of plastic. Different sectors consume plastics differently and this is influenced by the polymer type and lifetime of the end-product (Fig.1-3). The plastic packaging company in 2015 accounted for the half of the world plastic waste generated (efe-epa, 2018). Thermoplastics, mainly polyethylene (PE),

<sup>1</sup> From Fig.1-1, the blue colour indicates high recyclability, yellows show moderate recycling and red is non-recyclable.

polypropylene (PP), polyvinyl chloride (PVC), polystyrene (PS), polyamides (PA) and polyethylene terephthalate (PET), constitute of about 80% of the plastics consumed in Western Europe while the remaining 20% covers thermosets, mainly polyurethanes (PUR), amino-, phenolic-, and epoxy resins. (Nelson, 2017)

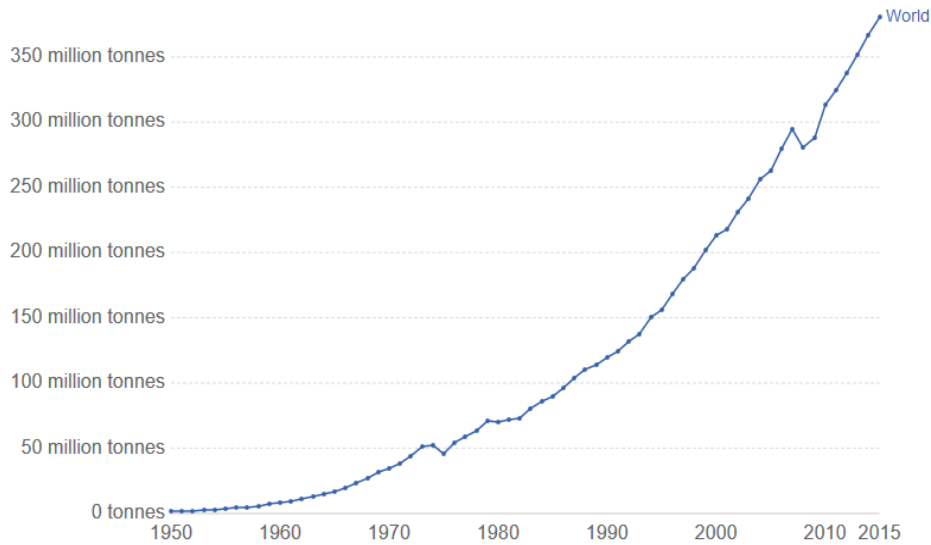


Figure 1-2: Global Plastics Production (Geyer, 2017)

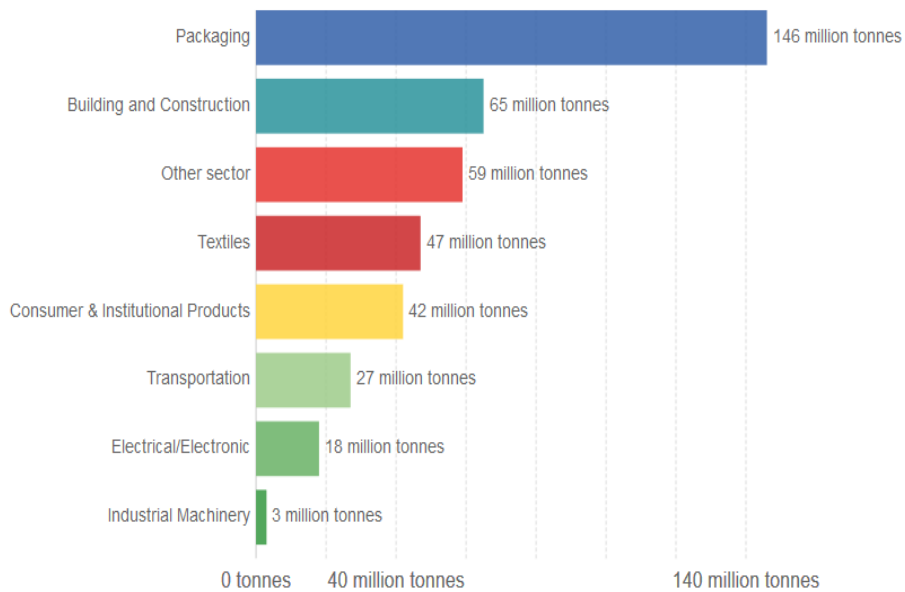


Figure 1-3: Plastic Consumption by Different Sectors (Geyer, 2017)

### 1.1.2 Plastic Waste Impact

Humans have become addicted to single use or disposable plastics which have adverse effect on our environment. Looking at the world today, 1 million plastic drinking water bottles are purchased every minute while about 5 trillion single use plastic bags are used worldwide annually. This simply means half of all plastics produced is designed to be used just once and thrown away. (Day, 2018) This is causing an adverse effect on our ecosystem.

### 1.1.2.1 Impact on Environment

**Oceans:** The distribution and accumulation of ocean plastics is strongly influenced by oceanic surface currents and wind patterns (Fig.1-4). Plastics are typically buoyant; thus, they can be easily transported by the prevalent wind and surface current routes. These plastics tends to accumulate in oceanic gyres, with high concentrations of plastics at the center of ocean basins and much less around the perimeters.

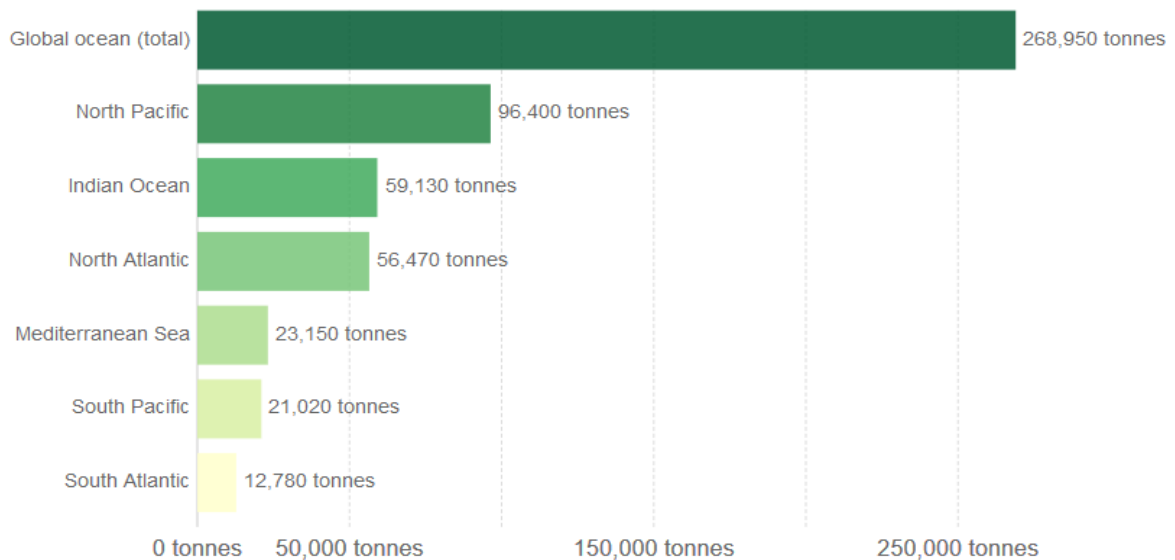


Figure 1-4 Surface plastic mass by ocean basin, 2013 (Eriksen, 2014)

**Land:** Plastics containing chlorine as additives, could release harmful chemicals into the soil which may later seep into groundwater, contaminating it. This could cause serious harm to living organism that drinks the water. Landfill as a form of waste management, contains different types of plastics. Microorganism, that facilitates the biodegradation of plastics, breaks this complex polymer, thereby releasing methane which is a greenhouse gas that severely contributes to global warming.

### 1.1.2.2 Impacts on Animals

On a yearly basis, ocean plastic is estimated to kill millions of marine animals. About 700 species including endangered ones are affected by this problem. Marine species of all sizes, from zooplankton to whales, now eat microplastics (Fig.1-5). Plastic wastes impact on wildlife is by three main pathways (Law, 2017). These are by entanglement, ingestion and interaction.



Figure 1-5 Plastic pollution in our world seas', and its effect on animals and humans (Arthur, 2017)

In 2004, a study was done on the gulls in the North Sea and it was discovered that these gulls had an average of about thirty pieces of plastic in their stomachs (Chris Wilcox, 2005). These animals mistake plastics floating on the sea as prey and probably ingest them thus, leading to these toxic chemicals like polychlorinated biphenyls (PCBs) in plastics to be released inside the bodies of these animals. These chemicals ingested could lead to destruction of digestive systems, reproductive system, weaken immune, malnutrition and death.

### 1.1.2.3 Impacts on Humans

Additives that are added in plastic production, may have harmful effect that could be carcinogenic or promote endocrine disruption. Additive such as phthalate plasticizers and brominated flame retardants via biomonitoring, have been identified in human population (Barnes, Galgani, Thompson, & Barlaz, 2009). Some chemicals in plastics has been deemed the leading cause of disruptions in fertility, reproduction, sexual maturation, and other health effects. (North & Halden, 2013)

## 1.2 Plastic Waste Management

The incitation of plastic waste management; recycling and incineration started around 1980 (Fig. 1-6), before then, after use, plastic waste was probably sent to landfill or discarded indiscriminately. During incineration of plastics, this process could lead to loss of oxygen and incomplete combustion may occur which may generate poisonous gases like dioxins and this can adversely affect human health. Due to the growing environmental concerns, landfill as a disposal process is being frowned upon and other methods such as gasification, pyrolysis and biodegradation seems like the best option.

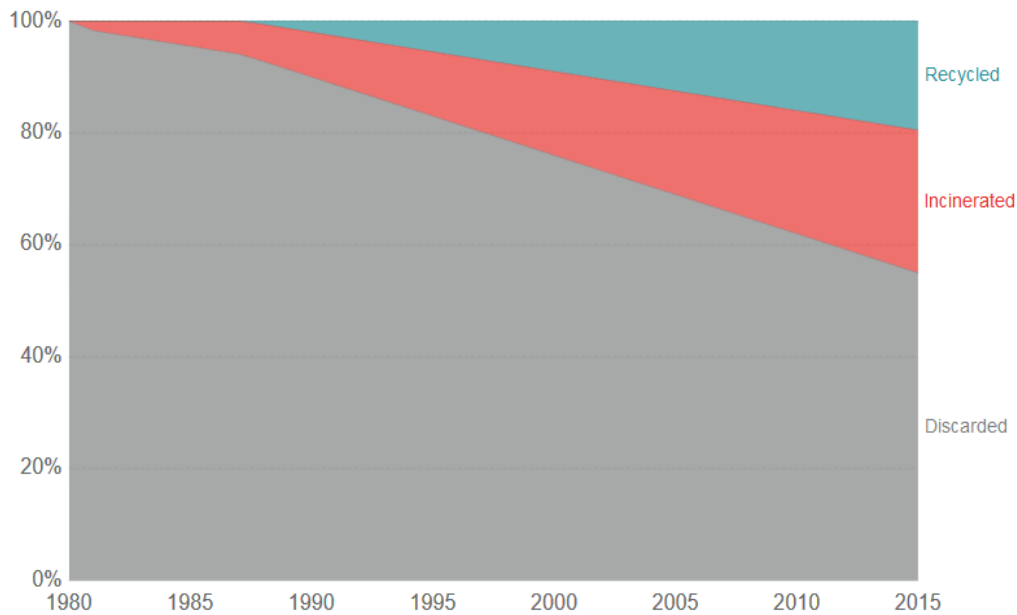


Figure 1-6 Global Plastic Waste by disposal (Geyer, 2017)

### 1.3 Plastic Waste to Energy

Energy plays an important role in the life cycle of plastics. Fossil fuels are used as feedstock to produce traditional plastics and energy is required for all the processes. With the increasing demand for energy, the world is faced with finding the right fuel that would not deplete finite stock but also reduce environmental concerns. At the end of the lifecycle of plastics, the energy used in the production should be recovered by appropriate waste management technique such that plastic waste is seen as a valuable material from the resources conservation's point of view and a good waste management can contribute to sustainable development.

Pyrolysis of waste plastic seems to be the most suitable method in terms of economics in solving the steadily increasing growing amount of plastic waste and meeting the growing energy demand. This is made possible by producing liquid fuel with similar properties to commonly use fossil fuel thereby limiting the world dependence finite hydrocarbon resources. HDPE, LDPE, PP and PS are polymers which contains hydrocarbon which shows similarity to hydrocarbon fuels. Plastics are produced from petroleum and their calorific value, is like those of LPG, petrol and diesel as shown in Table1-1 below.

Table 1-1: Comparison of energy density of plastics and different types of fuels (Baines, 1993)

Material	Calorific value (MJ/kg)
Polyethylene	46.3
Polypropylene	46.4
Polystyrene	41.4
Polyvinyl chloride	18.0
Coal	24.3
Liquefied petroleum gas	46.1

Petrol	44.0
Kerosene	43.4
Diesel	43.0
Light fuel oil	41.9
Heavy fuel oil	41.1

Pyrolysis is the thermochemical decomposition of large molecular weight polymer carbon in the absence of oxygen to produce smaller molecular weight fractions. This decomposition process may occur by removal of small molecules, depolymerization or random cleavage (Silvério, 2008). This process is usually endothermic thus, it requires the supply of heat for the reaction to occur (Buekens, 2006). Pyrolysis can be carried out at different temperatures, heating rate, reaction times, pressures, in the presence or absence of catalysts and reactive gases. The various operating conditions have a great influence on the type of product obtained and the volume of the yield. The product obtained includes gas, liquid consisting of paraffins, olefins, naphthenes and aromatics and solid (char).

Pyrolysis can be classified based on operating condition (heating rate); Fast pyrolysis leads to optimization of bio-oil production to about (60 – 70%), bio-char (15 – 25%) and Gas (10 – 15%) by increasing the rate of pyrolysis temperature to about 1000 °C/s. Slow pyrolysis uses a lower heating rate and the main product obtained from this process is bio-char.

Based on cracking mechanism of plastic pyrolysis, it can also be divided into thermal pyrolysis and catalytic pyrolysis. Thermal pyrolysis has to do with the degradation of polymer materials by the application of heat in the absence of oxygen. The temperature for this process, is between the range of 350°C to 900°C. Catalytic pyrolysis involves the use of a suitable catalyst, to carry out the degradation of the polymer material.

#### **1.4 Objectives**

HDPE, LDPE, PP, PS, and PET are the main constituents of municipal plastic waste. This thesis studied the thermal degradation of municipal plastic waste inclusive of ABS and NYLON with the aim of converting mixed plastic waste to energy. It is worth mentioning that although pyrolysis of plastic experimental analysis was not done due to certain constraints, however from the thermal degradation analysis the optimum temperature for mixed waste plastic pyrolysis was established, determination of kinetic parameters and simulation of pyrolysis for different heating rates was achieved.

Various research in literature, have shown that liquid yield obtained from mixed waste plastic pyrolysis was less than 50% due to different factors that influences pyrolysis process. However, the results obtained from this thesis can provide useful information for further studies in the optimization of the liquid yield of pyrolysis process for mixed plastic waste.



## 2 Thermal degradation of plastic waste

### 2.1 Polymer

Polymer is a word that was introduced by the Swedish chemist J. J. Berzelius (Dutton, 2018). He considered benzene ( $C_6H_6$ ) to be a polymer of ethyne ( $C_2H_2$ ). Polymers can thus be defined as natural or synthetic molecules that are composed of many smaller monomers (Fig.2-1) which have reacted to form a long chain.

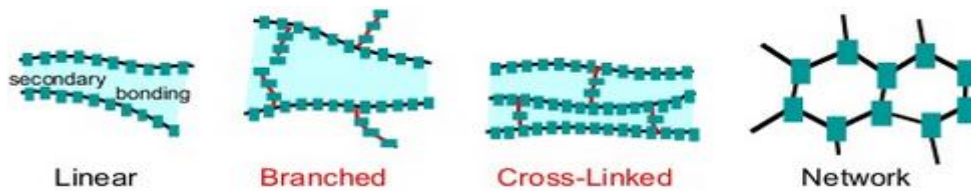


Figure 2-1 Polymer structures. (Dutton, 2018)

Polymers are classified by two major criteria which is according to its thermal behavior and polymerization mechanism. Plastics can be considered as equivalent to the term polymer. Nevertheless, all plastics are polymers, but not all polymeric materials are plastics. Polymers can be divided into three different groups:

- elastomers
- plastics
- fibers.

This classification is made based on their physical features, elastic modulus and degree of elongation.

**Plastics:** This means the ability to be shaped or molded by heat. Plastics can be sub-divided into different categories. These are:

- **Natural Plastics:** They are naturally occurring and can be shaped and molded by heat. An example is amber which is a form of fossilized pine trees resin and can be used in the manufacturing of jewelries.
- **Semi-Synthetic Plastics:** They are naturally occurring but have been modified by mixing them with other materials. An example is cellulose acetate which is obtained by the reaction of cellulose fibre and acetic acid and is used in the production of cinema film.
- **Synthetic Plastics:** These materials are obtained by the breaking down or cracking of carbon-based material (crude oil, coal or gas) with resulting changes in the molecular structure.

Semi- Synthetic and Synthetic plastics can be further divided into two categories. These categories are defined based on how the plastics react upon application of heat. These are:





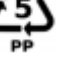

- **Thermoplastics:** This is formed by the application of heat and would assume the shape of the mold used during cooling.


- **Thermosetting plastics:** This would soften upon application of heat and can be molded when soft and when it cools, it sets into molded shape. However, upon re-application of heat, it would not re-soften because it is permanently in shape.

## 2.2 Chemical Composition of Plastics

Plastics are used for different purposes thus its composition may differ. These compositions are reported in terms of proximate analysis. Proximate analysis is a technique that is used in the determination of chemical properties of the plastic compound based on moisture content, fixed carbon, volatile matter and ash content (Kreith, 1998). Volatile matter and ash content are the major factors that influence the liquid and gas yield in pyrolysis process. High volatile matter indicates the high liquid oil production and a high ash content decreases the liquid production but increases the gaseous yield and char formation (Abnisa F, 2014). Table 2-1 shows the proximate analysis of different plastics. Based on the table, plastics have the possibility of producing liquid oil from the pyrolysis process based on its high volatile matter.

Table 2-1: Proximate Analysis of Plastics (Abnisa F, 2014)

Plastic Type	Plastic Type Mark	Moisture (wt%)	Fixed Carbon (wt%)	Volatile (wt%)	Ash (wt%)	Ref.
Polyethylene terephthalate (PET)		0.46	7.77	91.75	0.02	(Zannikos F, 2013)
		0.61	13.17	86.83	0.00	(Heikkinen JM, 2004)
High-density polyethylene (HDPE)		0.00	0.01	99.81	0.18	(Ahmad I. K., 2013)
		0.00	0.03	98.57	1.40	(Heikkinen JM, 2004)
Polyvinyl chloride (PVC)		0.80	6.30	93.70	0.00	(Hong S-J, 1999)
		0.74	5.19	94.82	0.00	(Heikkinen JM, 2004)
Low-density polyethylene (LDPE)		0.30	0.00	99.70	0.00	(Park SS, 2012)
		–	–	99.60	0.40	(Aboulkas A, 2010)
Polypropylene (PP)		0.15	1.22	95.08	3.55	(Jung S-H, 2010)
		0.18	0.16	97.85	1.99	(Heikkinen JM, 2004)
Polystyrene (PS)		0.25	0.12	99.63	0.00	(Abnisa F,

						2014)
		0.30	0.20	99.50	0.00	(Park SS, 2012)
Polyethylene (PE)		0.10	0.04	98.87	0.99	(Jung S-H, 2010)
Acrylonitrile butadiene styrene (ABS)		0.00	1.12	97.88	1.01	(Othman N, 2008)
Polyamide (PA) or Nylons		0.00	0.69	99.78	0.00	(Othman N, 2008)
Polybutylene terephthalate (PBT)		0.16	2.88	97.12	0.00	(Heikkinen JM, 2004)

### 2.3 Degradation Reaction Mechanism

Plastics thermal degradation is the breaking down of long polymer chains into smaller fractions and this process can be quite complex because it could be influenced by different factors. When plastics is subjected to high temperatures, its physical properties changes. Plastics undergoes three major thermal transitions with increasing temperature these are; glass transition, the melting, and decomposition as shown in (Fig.2-2). At room temperature, all polymers are hard solids, (glassy state.) As the temperature increases above glass transition temperature,  $T_g$ , the plastic gets enough energy to that allows the chains to move freely and becomes rubberlike (Wunderlich, 2005). As temperature further increases, the rubberlike plastic is changed to liquid-like substance when this temperature rises above the melting temperature,  $T_m$ , the plastic starts to decompose. When the decomposition temperature  $T_p$  is reached, the phenomena can be described by changes in elastic modulus of the plastics with the temperature increasing as shown in (Fig.2-3).

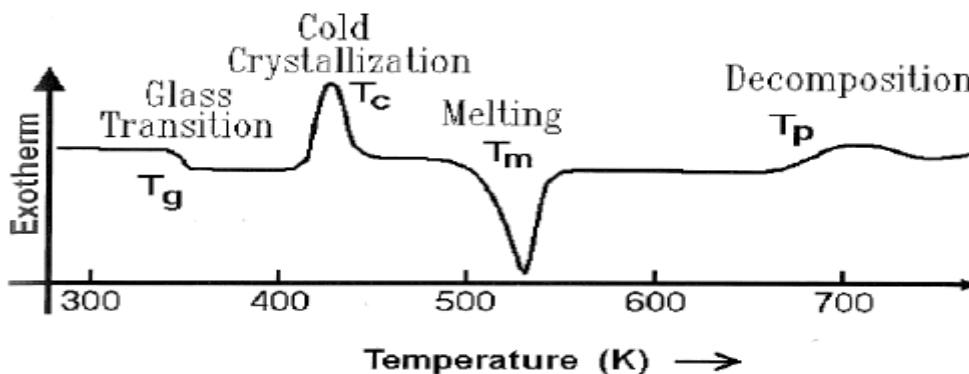


Figure 2-2 The phase transitions of PET by differential thermal analysis. (Wunderlich, 2005)

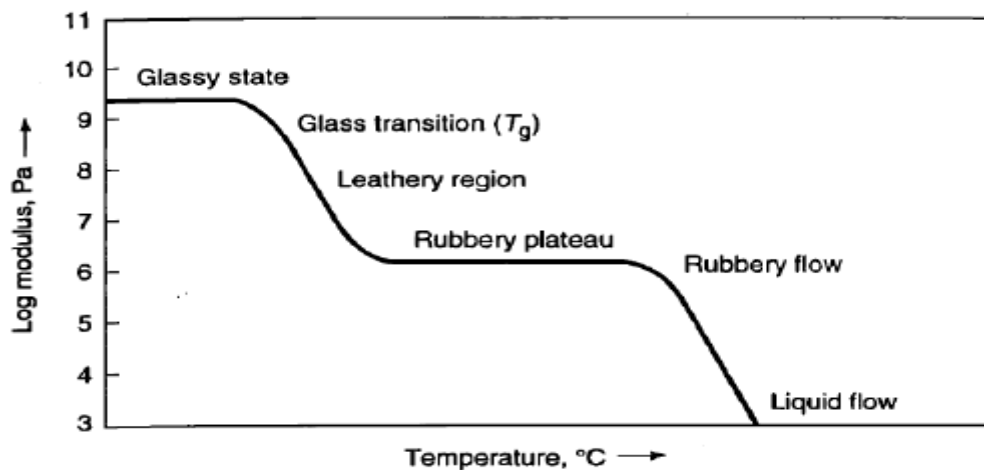


Figure 2-3 Effect of temperature on elastic modulus of polymers (Wade, 1995)

When the temperature rises above the plastics decomposition temperature, the plastics undergoes a chemical change which facilitate the cracking process. As the temperature keep increasing, vibration of the molecules keeps increasing until it gets to a point whereby it can overcome the Van der Waals force this process is called evaporation. However, if the induced energy due to the Van der Waals force is greater than the bond enthalpy between the molecules, cracking of the molecules would occur instead of evaporation. Cracking in the molecular structure generally occurs at the most unstable bonds. For plastics, differences in the carbon bond molecular structure influences the stability of the carbon bond as shown in (Fig.2-4) (Wade, 1995). Bond dissociation energy is the energy required to break bonds. This is the energy when the Van der Waals force induced energy is equal to the bond enthalpy. The bond dissociation energies for C-C bond of primary, secondary, and tertiary carbons are 355, 351, and 339kJ/mol, respectively (McMurry, 2000) .

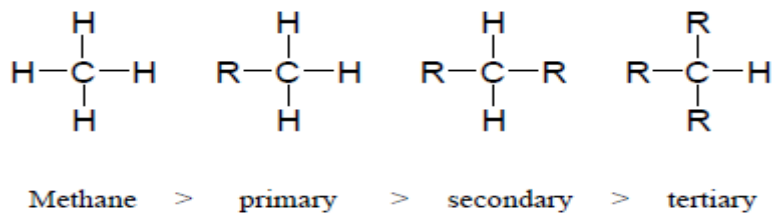


Figure 2-4 Stability of carbon bonds (Wade, 1995)

There are three types of cracking mechanism that occurs during plastic pyrolysis (Lee, 2006). These are:

- **Random cracking:** The carbon atoms, in linear plastics such as HDPE are on the long straight chains (secondary carbon) so the cracking on the carbon atoms of this polymer, have the same chance of occurring at anywhere. This is called random cracking (Saha, 2005) (Songip, 1994) (Levine, 2009). For tertiary carbon atoms at branched chains of LDPE, these bonds are less stable as compared to primary or secondary atoms thus the cracking would always occur first at the most unstable molecule. This is the reason why hydrocarbon obtained during the cracking of LDPE are straight chain as compared to those of linear HDPE. In PP, all the C-C bonds are on the tertiary carbon aside few C-C bonds at the ends of

PP molecules. This makes PP unstable as compared to PE. PP would probably produce smaller hydrocarbon as compared to PE. Random cracking is the main type of cracking in pyrolysis of PE, PP and PS.

- **Chain Strip Cracking:** In random cracking, the side carbon groups in the branched and cross-linked polymer units may come off the main carbon chains in the pyrolysis but in chain strip cracking, the unsaturated chain undergoes further reaction such as including cracking, aromatization and coke formation (Murty, 1996). This process in pyrolysis of polymer is usually carried out if polymer has a reactive side group.
- **End chain cracking**  
During cracking of plastics, the polymer could break from its end group if it is subjected to heating at or above the temperature of decomposition (Lee, 2006) (Murata, 2004)

## 2.4 Pyrolysis Reaction Stages

During plastic pyrolysis, numerous reactions are occurring but the four main reaction stages. These are initiation, propagation, hydrogen chain transfer and termination (Blazso, 2006) (Murata, 2004). The product type that is obtainable during plastic pyrolysis can be grouped into two; which are molecules (alkane, alkene etc.) and the free radical.

- **Initiation reaction:** In this reaction, the carbon chain of the polymer is broken to form smaller free radicals and molecules. This initial cracking can be done by either of the process in section 2.3 based on the polymer type. Initiation reaction produces lot of free radicals.
- **Propagation reaction:** This is the scission/cracking of the free radicals produced during the initiation reaction. Different studies have shown that  $\beta$ - scission is the main propagation reaction which includes both end chain scission and mid-chain scission. Propagation reactions during pyrolysis are intermediate reaction and it cracks large free radicals to produce alkene molecules and smaller free radicals.
- **Hydrogen chain transfer reactions:** This is proton transfer to other positions. The goal of this reaction is to reduce the molecular weight of the polymer (Chanda, 2000). Hydrogen chain transfer reaction can either be inter or intra molecular transfer reaction (Lee, 2006). Reaction between free radicals and other component is intermolecular transfer reaction. This type of reaction leads to the formation of saturated hydrocarbon molecules. Intramolecular transfer reaction is the transfer of free hydrogen proton from one end to the middle of the free radicals. This type of reaction results in isomer production in pyrolysis reaction.
- **Termination reaction:** This reaction occurs by the disproportionation of free radicals or the combination of two free radicals (Chanda, 2000) and it affects the product chain length. Thus, the product usually obtained from this type of reaction is usually large due to combination of free radicals from different plastics during pyrolysis.

### 2.4.2 Thermal Pyrolysis

In thermal pyrolysis, the polymer is subjected to high temperature which breaks it into smaller fractions ensuing in the formation of broad range of hydrocarbon. Higher temperature results in yield

containing non-condensable gases and lower liquid fractions. The duration of the reaction also plays an important role in the yield obtained (Scheirs, 2006). In thermal cracking, the stages involved in the mechanism are initiation, propagation and / or free radical transfer followed by  $\beta$  chain scission, hydrogen chain transfer and termination (Achilias, 2007) (Aguado, 2006)(Fig.2-5). Due to the high content of tertiary carbon of polypropylene (PP), the thermal cracking for polypropylene (PP) is less severe as compared to those for high density polyethylene (HDPE), followed by the low density (LDPE).

Initiation reaction is the homolytic breaking of the C-C bond. For PP and PE, the chain scission is random (Lee, 2006). In intermediate reaction, the radicals generated from initiation stage can be used to break the C-C bond by  $\beta$  scission to obtain compounds saturated or with unsaturated terminal and new radicals. Subsequent step is the hydrogen transfer reactions. During the hydrogen transfer from tertiary carbon atoms along the polymer chain to the radical site this mechanism yields many oligomers (Park D. W., 1999). The shifting of intra / intermolecular hydrogen is dependent on the experimental conditions. Firstly, it could lead to an increase in the increase production of olefins, and diolefins and subsequently increase paraffin production (Marcilla, 2009) (Aguado, 2006)

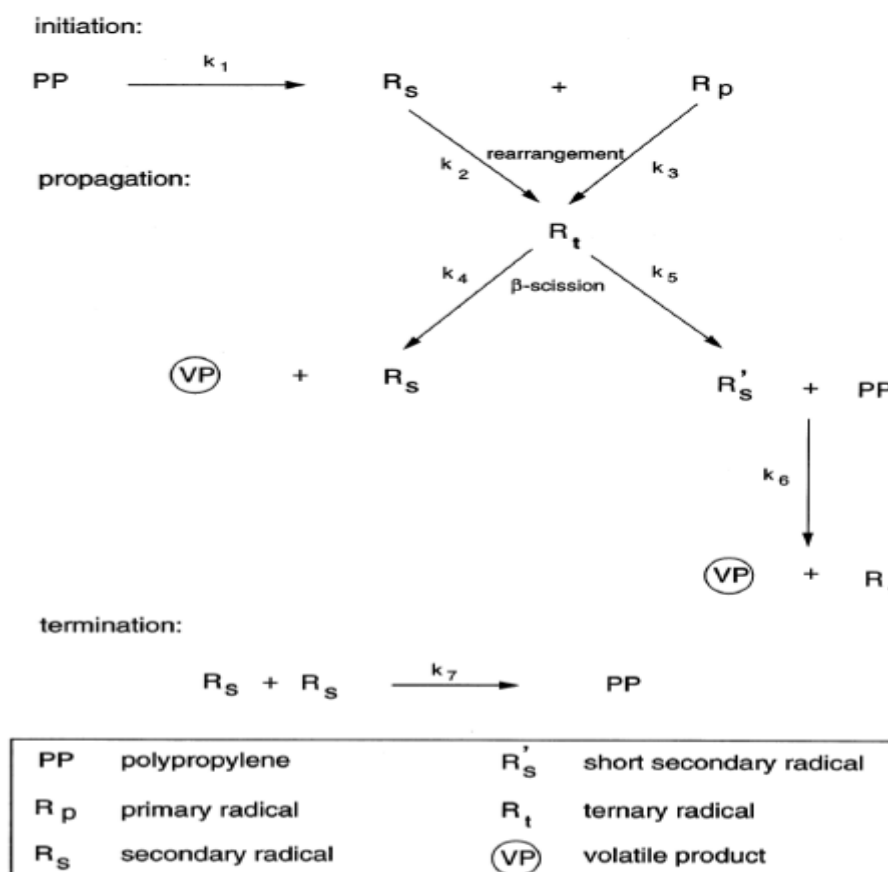


Figure 2-5 Radical mechanism of the thermal degradation of polypropylene (H. Bockhorn, 1999)

### 2.4.3 Factors Influencing Plastic Pyrolysis

In the optimization of product yield, different factors such structure of plastics and process parameters play a major role. In plastic pyrolysis, these key process parameters such as temperature, type of reactors, pressure, residence time, influences the products obtained.

- **Plastic Structure:** Plastics are classified based on the structural shape of the polymers. Thus, polymers can be linear, branched or crosslink polymer as shown in Fig 2-1. Linear polymer is a long continuous chain of carbon atom, while a branched chain polymer connects 3 or more branches on its main chain. Cross link polymer is an interconnected branched polymer with all its polymer chain linked to form a large molecule. Due to its large network structure, crosslink polymers cannot dissolve in solvent nor melt by application of heat. This type of polymers would rather crack and this is a different reaction process as compared to linear or branched polymer.
- **Temperature:** This is a fundamental parameter in plastic pyrolysis because it controls the cracking reaction of the polymer. Van Der Waal force holds molecules together and prevents disintegration. As the temperature of the system keep increasing, vibration of the molecules keeps increasing until it gets to a point whereby it can overcome the Van der Waals force this process is called evaporation. However, if the induced energy due to the Van der Waals force is greater than the bond enthalpy between the molecules, cracking of the molecules would occur instead of evaporation Table A-1, shows the different temperature for different type of polymer.
- **Heating Rate** It can be defined as the increase in temperature per unit time. In a research carried out by (Saha, 2005) on the influence of heating rate on the plastic pyrolysis of Pet bottle (Coca Cola). From the study it was observed that for PET polymer, increasing the heating rate promote the rate of the pyrolysis as shown in Fig 2-6 below.

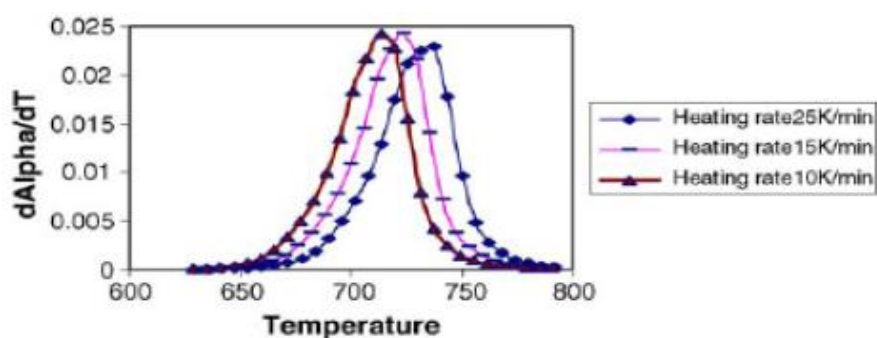


Figure 2-6 Reaction rate as a function of Temperature and heating rate in PET Pyrolysis (Saha, 2005)

- **Pressure:** This affects not just the pyrolysis reaction but also the product obtained from the process. The boiling point of the product obtained from plastic pyrolysis could increase with if the operating pressure is high. Thus, in a pressurized system heavier hydrocarbon fractions can undergo further pyrolysis instead of vaporization at a given temperature (Miranda, 2001)

(Murty, 1996) (Murata, 2004). In a study carried out by (Murata, 2004), he investigated the influence of pressure on the thermal degradation of PE polymer. From the studies, it was discovered that at higher pressure there was an increase the yield of non-condensable gas and a decrease in the yield of liquid product (Fig 2-7).

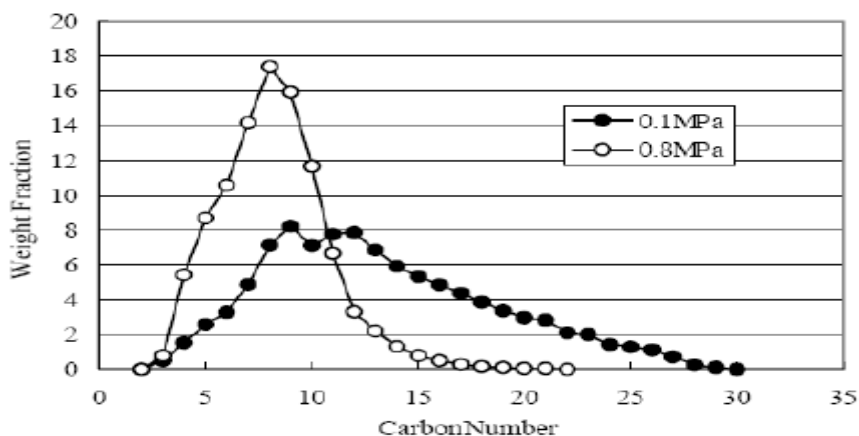


Figure 2-7 Influence of Pressure on the Distribution of Product from PE Pyrolysis (Murata, 2004)

- **Type of Reactor:** Reactor type in pyrolysis reaction, influences the mixing of plastics and catalyst, residence time, heat transfer and the overall efficiency of the reaction process. In lab scale, most plastic pyrolysis are performed using either batch or semi-batch and continuous flow reactor such as fixed bed, fluidized bed and conical spouted bed reactor. These different types of reactors have its specific advantages and disadvantages.
- **Residence Time:** This is the average time that a particle spends in the reactor and this parameter could influence the distribution of product. A longer residence time could result in a higher conversion of stable primary product such as non-condensable gas and light weight molecular product.

## 2.5 Development of Kinetic Models

There are different models that exist that can be used in the prediction of kinetic parameters based on weight loss experiment. Models differ in complexity and shows the variation of the mathematical function used in describing them. Various models have been suggested by different researchers in the literature and all are modelling is done based on kinetics. Kinetic models are mathematical functions developed from assumptions regarding reactants shape and the reaction driving force and these can be identified based on reaction mechanism. Degradation kinetics and pyrolysis mechanism is quite complex and is still being discussed and studied. To give a proper description of the decomposing mixture is difficult and much more in the presence of a catalyst

Thermogravimetry analysis (TGA) is a thermal analysis method that can help in the determination of weight loss and kinetics parameters as a function of temperature or time. It is the thermal degradation of sample in an inert condition at the same time, measuring the weight loss with increasing temperature while keeping the heating rate constant (Richardson, 2012). The instrument that is used for the continuous weighing of a sample as a function of temperature is the thermobalance and it



consist of recording balance, furnace, furnace temperature programmer or controller and recorder. As the temperature is increased, the products are formed during the scission of chemical bonds and non-isothermal experiments ends in complete conversion of the sample into degraded product with residue from carbon. The plot of weight vs temperature is called the thermogravimetric curve. Fig.2-8 shows non-isothermal TGA of plastics (PE, PP, PS and PMMA) in oxygen with a constant heating rate of 5°C/min for about two hours.

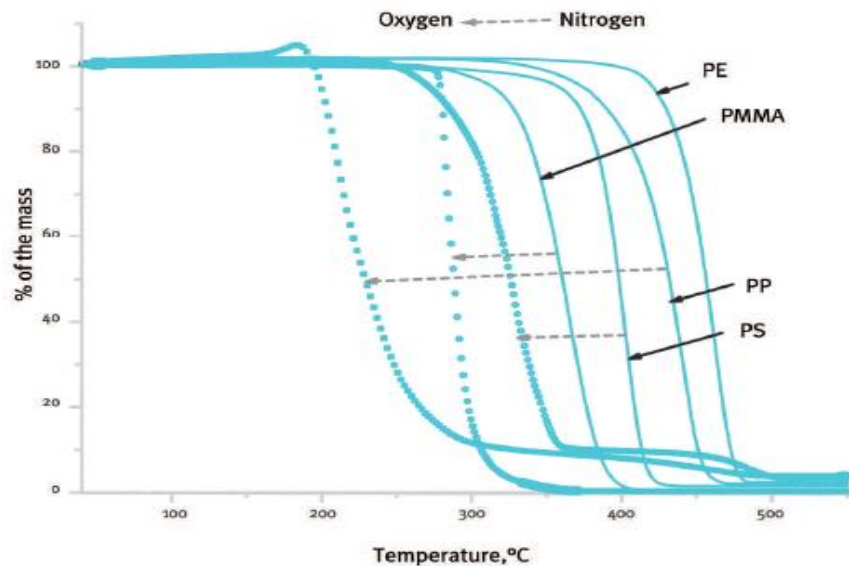


Figure 2-8 Non-Isothermal Thermogravimetric analysis of plastics (Richardson, 2012)

### 2.5.1 Thermogravimetric Curve

The thermogravimetric curve (Fig 2-8) generated from the results of heating of a sample at constant temperature can give direct insight into the number of stages of decomposition and the fractional weight-loss of each stage. The thermogravimetric curve is shaped by many factors, like design of the crucible, heating rate, sample form and sample weight. Chemical reactions are temperature-dependent rate reactions; which means sample weight-reduces over time when exposed to range of temperatures. Since rate of weight-loss and heating rate are dynamic processes, weight-loss curves will shift along the temperature axis when obtained at different constant heating rates. On a thermogravimetric curve, the following features may be identified:

- A plateau or table portion, which is indicative of constant weight.
- A curved portion, the steepness of which is indicative of the rate of weight-loss and will pass through a maximum.
- A trough portion indicative of the formation of an intermediate compound.

A DTG curve comprises of a chain of peaks coinciding to the various stages in the decomposition process, with the maximum peak being equivalent to the inflection point of the TG curve, and the peak area being proportional to the fractional weight-loss at each stage. The curve goes back to the baseline when the plateau region once the sample weight reaches a plateau.

### 2.5.2 Factors Influencing Thermogravimetry Analysis

- **Sample Size and Geometry:** How solids behave upon application of heat is influenced by differences in its structure such as defect content, porosity and surface properties. Increase in the amount of the sample, causes temperature to become non-uniform through slow heat transfer as the reaction occurs. The degree of diffusion of the product gas through void spaces is affected by the sample size. Ideally, it is preferable that the sample's weight is as small as possible within limits of balance sensitivity. Different studies on thermogravimetry analysis, samples are usually in powdered form. This is because the smaller the particle size, the greater the extent to which equilibrium is reached, and at any given temperature, the extent of decomposition was found to be greater. Thus, grain size, grain size distribution and closeness of the size fraction influences the thermogravimetric curve obtained.
- **Atmospheric Effect:** Draughting, buoyancy and convection effects can influence the weight changes when thermogravimetric analysis is out under flowing gas conditions. Draughting effects arise when stream of gas molecules flows unidirectionally past the sample container. Increase in furnace temperature has been found to decrease buoyancy effect. High frequency aerodynamic noise can be as a result of convection currents, turbulence and the flow of the atmosphere. Increase in temperature could slightly increase the amplitude. A constant gas flow will still produce a constant error, and this cannot be neglected.
- **Heating Rate:** During thermogravimetric analysis, if fast heating rate is employed, a polymer decomposing in one step will seem like it has an initial temperature of decomposition higher than its true initial temperature. This is as a result of finite time needed to cause a noticeable weight change. Thus, at any given temperature, the extent of decomposition is greater at a slow heating rate when compared to a similar sample heated at a fast heating rate.

### 2.5.3 Kinetics Analysis of Thermogravimetric Data

Reaction kinetics focus on the study of the speed of chemical reactions and how they are influenced by different factors such as reactants concentration, pressure and temperature. How these factors influences the reaction, is dependent on the reaction mechanism which describes the individual steps in a reaction sequence. To understand the reaction mechanism, these factors and its rate allows for the possibility to influence these steps during conversion process (WOJCIECHOWSKI, 2003).

Temperature is an important factor that helps in explaining the mechanism of chemical kinetic because it influences the rate of change. Arrhenius equation is a formula that is based on the temperature dependence of reaction rate. Svante Arrhenius proposed this equation in 1889 based on work of Jacobus Henricus van 't Hoff a Dutch Chemist in 1884 where he proposed an equation for temperature dependence of equilibrium constants and proposed a formula for the rate of both forward and reverse reaction. This equation helps in the determination of rate of chemical reaction and activation energy (Arrhenius, 1889). Based on Arrhenius ability to provide physical justification and interpretation of this formula, it can now be used in modelling of temperature variation of coefficients, population of crystal vacancies, creep rates, and many other thermally-induced processes/reactions.

Kinetics for degradation reaction process can either be isothermal or non-isothermal. Isothermal reaction occurs when the system temperature is rapidly raised to a pre-determined experimental temperature and the system heating occurs so fast which does not give enough time for the main degradation reaction to occur. Once the set temperature is reached, main degradation reaction takes place, temperature remains constant while time changes as the reaction proceeds. For non-isothermal reaction, the heating process of the system is much slower as compared to isothermal process hence this allows for the degradation reaction to take place during the heating process of the system as the temperature increases.

For this study, the TGA experiments were carried out in non-isothermal condition, meaning the devolatilization of the samples occurred at non-constant temperature with constant pressure. Rate of decomposition is dependent on temperature  $T$  and  $\alpha$ .  $\alpha$  describes the overall transformation that the reactant progresses. This transformation process involves numerous reactions, each with its specific extent of conversion. Thus,  $\alpha$  can be described as the conversion which is calculated from total weight loss and is defined as follows (VYAZOVKIN, et al., 2011):

$$\alpha = \frac{m_o - m_T}{m_o - m_f} \quad (2.1)$$

Where;

- $m_o$  is the initial sample mass (kg);
- $m_T$  is the remaining sample mass at temperature  $T$  (kg); and
- $m_f$  is the final mass (kg).

Thus, in thermogravimetric analysis, thermal decomposition of feedstock under above stated conditions can be defined as:

$$\frac{d\alpha}{dt} = K(T) f(\alpha) \quad (2.2)$$

Where;

- $K(T)$  is the temperature dependent rate constant
- $f(\alpha)$  is the conversion function dependent on the reaction mechanism.
- $d\alpha/dt$  is the transformation rate

Rate constant can be defined by Arrhenius equation as follows:

$$K(T) = A e^{-\left(\frac{E}{RT}\right)} \quad (2.3)$$

Where;

- $A$  is the pre-exponential factor or frequency factor ( $\text{min}^{-1}$ );
- $E$  is the activation energy of the decomposition reaction (kJ/mol);
- $R$  is the universal gas constant (8,314 J/mol.K);
- $T$  is the absolute temperature (Kelvin)

The activation energy  $E$  can be defined as the minimum energy required to activate molecules and atoms to a state where they can undergo chemical reaction. It is also the difference between the reactants state and transition state. It can also be described as the minimum amount energy required by molecules to break existing bonds during chemical reaction. Thus, for chemical reaction to take place, it is the least amount of energy that is required to be in place. The highest energy state of a system in chemical reaction is the transition state. In reactants state, if the molecules collision occurs, enough kinetic energy is required to overcome this energy barrier for reaction to occur and product to be formed. Thus, the higher the activation energy, the harder it is for chemical reaction to occur and lower activation energy makes it easier for reaction to take place (WOJCIECHOWSKI, 2003) .

The pre-exponential factor or the frequency factor is the frequency of collision between the molecules of the reacting compounds. This frequency is proportional to the product of the concentration's product (WOJCIECHOWSKI, 2003)

Thus, combining equation (2.2) and (2.3) produces the basic expression for the study of kinematics of heterogeneous solid-state thermal decomposition

$$\frac{d\alpha}{dt} = A e^{-\left(\frac{E}{RT}\right)} f(\alpha) \quad (2.4)$$

Similarly, the decomposition rate equation can be written as

$$\frac{d\alpha}{dT} = \frac{d\alpha}{dt} \frac{dt}{dT} \quad (2.5)$$

Where;

- $\beta = \frac{dT}{dt}$  is the heating rate (K/min);

Simplification of equation (2.4) is not possible in non-isothermal experiment carried out under non-constant heating rate. However, for non-isothermal experiment with linear and constant heating rate which was developed for this study, equation (2.5) can be written as:

$$\frac{d\alpha}{dT} = \frac{d\alpha}{dt} \frac{1}{\beta} \quad (2.6)$$

Therefore, by the application of equation (2.6), the decomposition rate equation can be expressed as function of temperature

$$\frac{d\alpha}{dT} = \frac{A}{\beta} e^{-\left(\frac{E}{RT}\right)} f(\alpha) \quad (2.7)$$

Thus, equation (2.7) can be used in describing the thermal decomposition of the feedstock for non-isothermal TGA experiments with constant heating rate, written in function of the reaction mechanism,  $f(\alpha)$ . This equation represents the differential form of the non-isothermal rate law, and it can be applied in the calculation of kinetic parameters of feedstock.

### 2.5.2.1 Determination of Kinetic Parameters

The methods used for kinetic analysis of decomposition process can be divided into two main groups model fitting kinetics and model free kinetics methods (KHAWAM, 2007). Model fitting method chooses the kinetic model and estimates the values of model parameters by fitting on experimental data. Some of the most used such methods include Freeman-Carroll, Coats-Redfern, Fătu, Reich-Levi or the initial rate method (Dumitrașă, 2014). In model free methods no assumption of specific reaction model and yields kinetic parameters as a function of either conversion (isoconversional analysis) or temperature (non-parametric analysis) (VYAZOVKIN, et al., 2011). Isoconversional methods are based on isoconversional principles which states that the constant extent of conversion is a function of solely temperature. Application of isoconversion method, require running the experiment using different heating rates; so, this method was decided not to be used in the calculation of the activation energy for this study considering that only one heating rate was obtained. The methods used are:

- **Assumption of the degradation mechanism f(α):** Modelling the thermal decomposition of some solid feedstock that have not been modelled, the automatic assumption of the degradation mechanism or the f(α) conversion function, would be something quite unimaginable or beyond one's means. However, based on different publications where thermal degradation analysis of polymer is studied, the conversion function f(α), which is dependent on the reaction mechanism, is assumed to be as follows (Alonso, 2016)

$$f(\alpha) = (1 - \alpha)^n \quad (2.8)$$

Where;

- n is the reaction order of the decomposition process.

Substituting equation (2.8) in the general differential equation of the non-isothermal rate law presented by equation (2.7), the following expression is obtained:

$$\frac{d\alpha}{dt} = \frac{A}{\beta} e^{-\left(\frac{E}{RT}\right)} (1 - \alpha)^n \quad (2.9)$$

Equation (2.9) shows the degradation reaction of polymers. The decomposition rate of plastics at any given temperature depends on the fraction of plastics that has not reacted at that point (1-α), together with the reaction order, n. This equation will be employed in the calculation of kinetic parameters of the samples.

- **When: n=1:** If first order reaction mechanism is assumed, which implies that the assumed conversion function f(α) = (1-α)<sup>n</sup> for the thermal decomposition of plastics, the equation describing the reaction rate of the decomposition process will consist of:

$$\frac{d\alpha}{dt} = \frac{A}{\beta} e^{-\left(\frac{E}{RT}\right)} (1 - \alpha) \quad (2.10)$$

Thus, for this case the unknown parameters are the activation energy, E, and the pre-exponential factor, A, as the reaction order has already been assumed to be 1. This

assumption of first order reaction mechanism is widely applied in the available literature for describing the decomposition of plastics (Alonso, 2016).

- **Graphical approach:** To determine the activation energy, the pre-exponential factor and the order of reaction, this approach uses two different graphical methods that assumes the conversion function as  $f(\alpha) = (1-\alpha)^n$ . Each of these methods gives slightly different kinetic parameters.

- **Direct Arrhenius Plot Method:** This method, is based on taking the logarithm of equation (2.9), thus the following expression is obtained (Alonso, 2016):

$$\ln \left[ \frac{1}{(1-\alpha)^n} \frac{\partial \alpha}{\partial T} \right] = \ln \left( \frac{A}{\beta} \right) - \left( \frac{E}{RT} \right) \quad (2.11)$$

For further simplification, and evaluation of the parameters and so that the graphical expression of equation (2.12) could be easier to achieve, the following X and Y parameters are defined:

$$Y = \ln \left[ \frac{1}{(1-\alpha)^n} \frac{\partial \alpha}{\partial T} \right] \quad (2.12)$$

$$X = \frac{1}{T} \quad (2.13)$$

So, equation (2.11) will result in:

$$Y = \ln \left( \frac{A}{\beta} \right) - \left( \frac{E}{R} \right) X \quad (2.14)$$

- **Coats and Redfern:** This is a method for estimating kinetic parameters using an integrated form of the rate equation which is expressed in equations (2.15) & (2.16) depending on the assumption of n-order kinetics ( $n \neq 1$ ) or the assumption of first order reaction mechanism ( $n=1$ ). (Mostafa ME, 2015)

**For  $n \neq 1$ :**

$$\ln \left[ \frac{1 - (1-\alpha)^{1-n}}{T^2(1-n)} \right] = \ln \left( \frac{AR}{\beta T} \right) - \frac{E}{RT} \quad (2.15)$$

**For  $n=1$ :**

$$\ln \left[ \frac{-\ln(1-\alpha)}{T^2} \right] = \ln \left( \frac{AR}{\beta T} \right) - \frac{E}{RT} \quad (2.16)$$

Thus, Y and X notation for each case, can be defined as:

**For  $n \neq 1$ :**

$$Y = \ln \left[ \frac{1 - (1-\alpha)^{1-n}}{T^2(1-n)} \right] \quad (2.17)$$

$$X = \frac{1}{T} \quad (2.18)$$

**For  $n=1$ :**

$$Y = \ln \left[ \frac{-\ln(1 - \alpha)}{T^2} \right] \quad (2.19)$$

$$X = \frac{1}{T} \quad (2.20)$$

- **Horowitz and Metzger:** This approach assumes that during pyrolysis reaction, no intermediates are formed, all products are gases, which escaped immediately. This model is based on a combination of the reaction rate dependence on both concentration and temperature. Reaction rate dependence on concentration is given by:

$$\frac{dC}{dt} = -KC^n \quad (2.21)$$

Where;

- C is concentration (mole fraction or amount of reactant)
- k is specific rate constant
- n is order of reaction
- t is time

The equation (2.21) above shows that the rate of disappearance of reactant, per unit volume or per unit total weight or per unit total moles, as a power function of the concentration of reactant:

$$\frac{dW}{W_t dt} = -KC^n \quad (2.22)$$

Where,

- W is the weight or number of moles of reactant
- $W_t$  is the total weight at any time

Based on the assumption that all gaseous products escape immediately, it can be said that the concentration is constant throughout the pyrolysis ( $C = 1$  on a weight or mole fraction basis). For pyrolysis, the total change in concentration is due to the decrease of weight (W) as well as the change in total weight due to the loss of reactant and accumulation of products.

$$\frac{dW}{W_t dt} = -Ae^{-\left(\frac{E_a}{RT}\right)} C^n \quad (2.23)$$

The order of reaction in solid state reactions generally has no significance and  $C = 1$ , thus, equation (2.23) becomes:

$$\frac{dW}{W_t dt} = -Ae^{-\left(\frac{E_a}{RT}\right)} \quad (2.24)$$

Where

- $W = W_t =$  sample weight.

If  $q$  is defined as the rate of temperature rise ( $dT/dt = q$ ), then:

$$\ln \frac{W}{W_0} = \int_0^T \frac{A}{Q} e^{-\left(\frac{E_a}{RT}\right)} dT \quad (2.25)$$

Where

- $W_0$  is the initial weight.

Most pyrolysis take place at a narrow temperature range and at a relatively high absolute temperature. Thus, a reference temperature,  $T_s$ , can be defined, such that at  $T_s$ ,  $W/W_0 = 1/e$ .

Defining  $\theta$  such that  $T = T_s + \theta$ , then

$$\frac{1}{T} = \frac{1}{T_s + \theta} = \frac{1}{T_s \left(1 + \frac{\theta}{T_s}\right)} \quad (2.26)$$

Since  $\theta/T_s \ll 1$ :

$$\frac{1}{T} \cong \frac{1 - \frac{\theta}{T_s}}{T_s} \quad (2.27)$$

Substituting equation (2.27) into equation (2.25) and then integrating gives:

$$\ln \frac{W}{W_0} = -\frac{A}{Q} \frac{RT_s^2}{E_a} e^{-\left(\frac{E_a}{RT}\right)\left(1 - \frac{\theta}{T_s}\right)} \quad (2.28)$$

When  $T=T_s$ ,  $\theta=0$ ,  $W/W_0 = 1/e$  and  $\ln W/W_0 = -1$ .

Thus, when  $\theta = 0$ , equation (2.28) becomes:

$$-1 = -\frac{A}{Q} \frac{RT_s^2}{E_a} e^{-\left(\frac{E_a}{RT}\right)} \quad (2.29)$$

Substituting equation (2.29) for the corresponding part of equation 2.28:

$$\ln \frac{W}{W_0} = -e^{-\left(\frac{E_a \theta}{RT_s^2}\right)} \quad (2.30)$$

or

$$\ln \ln \frac{W}{W_0} = -\frac{E_a \theta}{RT_s^2} \quad (2.31)$$



- **Distributed Activated Energy Method:** This model, assumes that pyrolysis of complex material is a first order decomposition with different chemical group and each group is characterized by its own unique activation energy for the decomposition process (Fakir, 2012). In this model, the activation energy is said to follow a distribution function along the degradation process. The most commonly used distribution function is Gaussian distribution. General equation for DAEM is as follows (Scott, 2006):

$$1 - \frac{V}{V^*} = X = \int_0^{\infty} \exp(-A \int_0^t e^{-\frac{E_0 t}{RT}} * \delta t) f(E) \delta E \quad (2.32)$$

Expressing equation (2.32) as a function of temperature gives

$$1 - \frac{V}{V^*} = X = \int_0^{\infty} \exp(-\frac{A}{\beta} \int_0^t e^{-\frac{E_0 t}{RT}} * \delta t) f(E) \delta E \quad (2.33)$$

Where

- f(E) is the distribution function of activation energy
- X is the ratio of volatile that is released at specific temperature to the total volatile released
- V is the total volatiles released
- V\* is the volatile released at a specific temperature

Since Gaussian activation energy distribution is assumed, f(E) can be defined as:

$$f(E) = \frac{1}{\sigma\sqrt{2*\pi}} \exp(-\frac{(E-E_0)^2}{2\sigma^2}) \quad (2.34)$$

Defining equation (2.34) in terms of terms V and V\* yields

$$1 - \frac{V}{V^*} = \frac{V^* - V}{V^*} = \frac{m_T - m_f}{m_0 - m_f} = \alpha \quad (2.35)$$

From equation (2.1),  $\alpha$  can be defined as  $\alpha = \frac{m_0 - m_T}{m_0 - m_f}$ , thus, rearranging equation (2.35) gives:

$$1 - \alpha = X \quad (2.36)$$

DAEM is quite a complex method in determination of kinetic parameters and the complexity lies in the double integration the general equation hence it is difficult to find an exact mathematical solution. Because of this complexity, obtaining the kinetic parameters can either be by distribution free or distribution fitting.

### 3 Materials and Methods

#### 3.1 Materials

##### 3.1.1 Plastics

For this study, the plastics obtained comprises of disposable cups, Coca-Cola bottle, drinking water bottles, different kinds of plastics bags, straws, cover of water bottles and disposable spoons and fork obtained from municipal solid waste (MSW) of Portuguese households. Reference polymer materials (PET, LDPE, PS, NYLON & ABS) was obtained from a plastic company. The plastics was washed, dried and sorted accordingly as shown in Fig.3-1 below. Fourier Transform Infrared Spectroscopy (FTIR) was used in the characterization of the plastics and its corresponding spectra was compared with the results obtained from municipal solid plastic waste and literatures

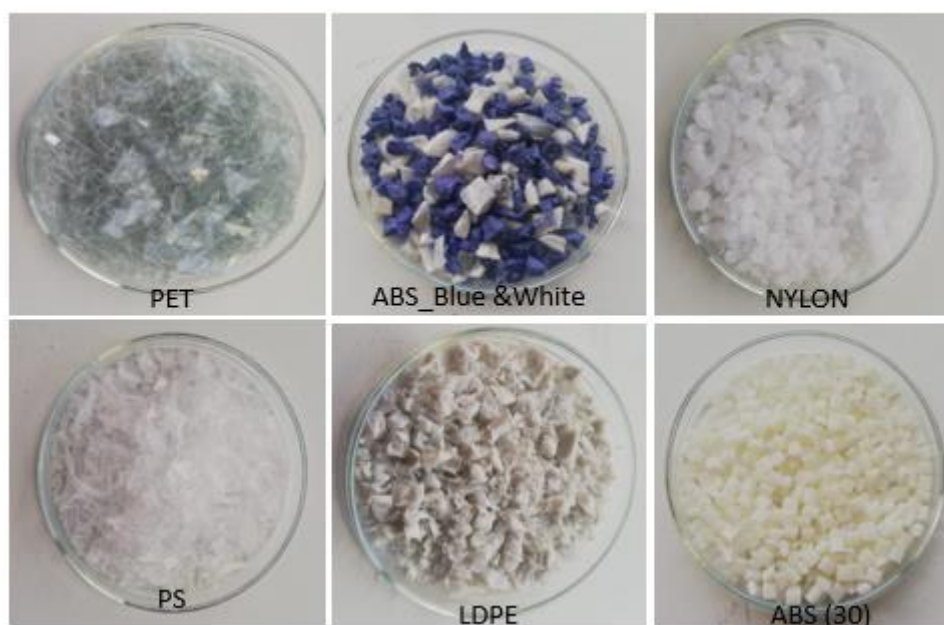


Figure 3-1 Plastic Waste

#### 3.2 Plastic Characterization

##### 3.2.1 Fourier Transform Infrared Spectroscopy (FTIR)

Infrared spectroscopy is an important characterization technique which shows matter structure on a molecular level. Compounds chemical composition and bonding can be obtained using Infrared spectroscopy.

Based on the Fourier transformation of signal from an interferometer, the FTIR spectrometer obtains the IR spectrum. The spectrum can operate in transmission, reflection and in attenuated total reflection mode (ATR) This is a technique that is based on the absorption of infrared photon that excite vibration of molecular bonds (EAG, 2014). It generates a spectrum with a characteristics band that helps in the identification and characterization of samples. To analyze a spectrum, a knowledge of the

functional group is necessary. Table 3-1 shows the key functional groups and wavelength used in the identification of the plastics for this study.

Table 3-1: Functional Groups and Component Classes in the FTIR Spectrum for Polymer Material

Wavelength (cm <sup>-1</sup> )	Functional group	Polymer	Reference
1713 (a) 1241 (b) 1094 (c) 720 (d)	C=O stretch C-O stretch C-O stretch Aromatic CH out of plane bend	PET	(Asensio, 2009) (Verleye, 2001) (Noda, 2007)
2915 (a) 2845 (b) 1472 (c) 1462 (d) 730 (e) 717 (f)	C-H stretch C-H stretch CH <sub>2</sub> bend CH <sub>2</sub> bend CH <sub>2</sub> rock CH <sub>2</sub> rock	HDPE	(Asensio, 2009) (Noda, 2007) (Nishikida, 2003) (Coates, 2000)
1427 (a) 1331 (b) 1255 (c) 1099 (d) 966 (e) 616 (f)	CH <sub>2</sub> bend CH bend CH bend C- C stretch CH <sub>2</sub> rock C-Cl stretch	PVC	(Beltran, 1997) (Verleye, 2001) (Noda, 2007)
2915 (a) 2845 (b) 1467 (c) 1462 (d) 1377 (e) 730 (f) 717 (g)	C-H stretch C-H stretch CH <sub>2</sub> bend CH <sub>2</sub> bend CH <sub>3</sub> bend CH <sub>2</sub> rock CH <sub>2</sub> rock	LDPE	(Asensio, 2009) (Coates, 2000) (Nishikida, 2003) (Noda, 2007)
2950 (a) 2915 (b) 2838 (c) 1455 (d) 1377 (e) 1166 (f) 997 (g) 972 (h) 840 (i) 808 (j)	C-H stretch C-H stretch C-H stretch CH <sub>2</sub> bend CH <sub>3</sub> bend CH bend, CH <sub>3</sub> rock, C-C stretch CH <sub>3</sub> rock, CH <sub>3</sub> bend, CH bend CH <sub>3</sub> rock, C-C stretch CH <sub>2</sub> rock, C-CH <sub>3</sub> stretch CH <sub>2</sub> rock, C-C stretch, C-CH stretch	PP	(Asensio, 2009) (Verleye, 2001) (Noda, 2007)
3024 (a) 2847 (b) 1601 (c) 1492 (d) 1451 (e) 1027 (f) 694 (g)	Aromatic C-H stretch C-H stretch Aromatic ring stretch Aromatic ring stretch CH <sub>2</sub> bend Aromatic CH bend Aromatic CH out of plane bend	PS	(Asensio, 2009) (Verleye, 2001) (Noda, 2007)

2922 (a) 1602 (b) 1494 (c) 1452 (d) 966 (e) 759 (f) 698 (g)	C-H stretch Aromatic ring stretch Aromatic ring stretch CH <sub>2</sub> bend =CH-bend Aromatic CH out of plane bend, =CH bend Aromatic CH out of plane bend	Acrylonitrile butadiene styrene (ABS)	(Verleye, 2001)
3298 (a) 2932 (b) 2858 (c) 1634 (d) 1538 (e) 1464 (f) 1372 (g) 1274 (h) 1199 (i) 687 (j)	N-H stretch CH stretch CH stretch C=O stretch NH bend, C-N stretch CH <sub>2</sub> bend CH <sub>2</sub> bend NH bend, C-N stretch CH <sub>2</sub> bend NH bend, C=O bend	NYLON	(Noda, 2007)

### Procedure

The FTIR trials for the different plastic samples was conducted using the Perkin-Elmer Spectrum Two FT-IR Spectrometer Two Universal ATR (Fig 3.2). The spectra collected was set from 4000 cm<sup>-1</sup> to 600 cm<sup>-1</sup> with a data interval of 1 cm<sup>-1</sup>. Resolution was set at 4 cm<sup>-1</sup>.

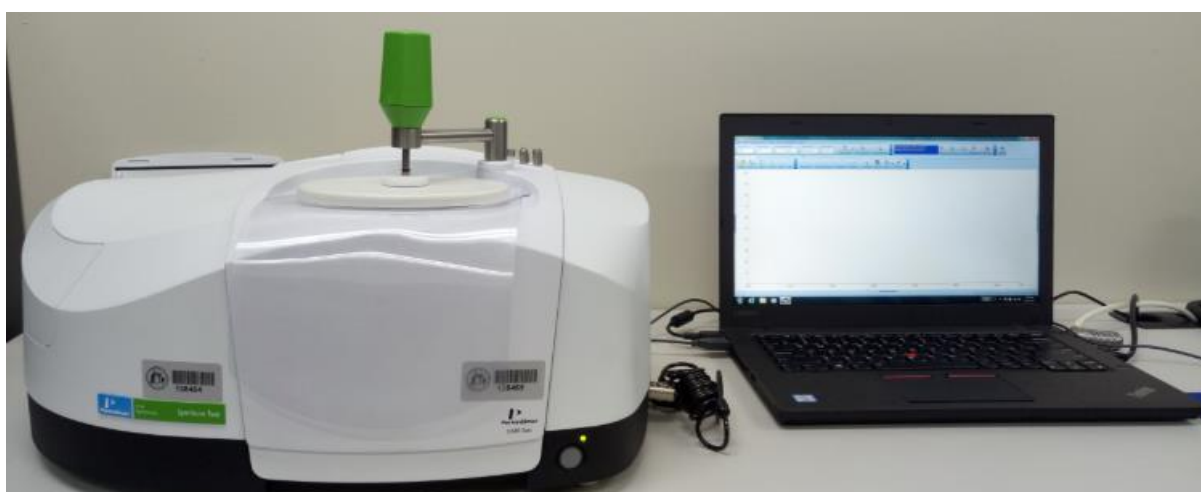


Figure 3-2 Perkin-Elmer Spectrum Two FT-IR Spectrometer

The steps for conducting the FTIR trials were:

1. The computer was turned on
2. The equipment was turned on
3. The software (Spectrum IR) was opened from the desktop
4. The analysis set up (wavenumber range from and number of scans) from the software toolbar were selected
5. The sample holder was cleaned properly with acetone using wipes.

6. The sample was placed properly on the sample holder with a force of about 80 N to ensure good contact between sample and ATR crystal
7. From the software toolbar, the scan button was clicked first, then clicked again to set the force gauge.
8. The spectrum was generated
9. The sample name was changed by clicking the left side of the software which brought up a dialogue box where the sample name was change accordingly.
10. The old sample was removed, sample holder cleaned a new sample was placed and steps 5,6,7 and 8 were repeated.
11. After the trials, the software was turned off, computer logged off and the machine was switched off.
12. The sample holder was cleaned properly
13. All data obtained by FTIR was treated by the Kubelka-Munk method. It is a method that decreases the noise. It can express by the equation below;

$$I_{corrected} = \frac{(1-R)^2}{2R} \quad (3.1)$$

Where,

- R = reflectance
- I = intensity

### 3.2.1 Thermogravimetric Analysis (TGA)

Thermogravimetric analysis of plastics was carried out using TG-DTA/DSC sateram labsys (Fig 3.3) in Nitrogen atmosphere. The experimental trials was initiated at a temperature of 25°C with heating rate of 30°C/min and ended at about 1100°C.



Figure 3-3 TG-DTA/DSC Sateram labsys

### 3.2.1.1 Determination of Kinetic Parameters

#### Direct Arrhenius Plot Method

- **Determining the order of reaction, n** (Alonso, 2016)

Plotting the parameters Y and X from equation (2.12) and (2.13), the order of reaction n, can be obtained as follows:

- Y parameter defined by equation (2.12) would be analyzed alongside values of parameter X (equation (2.13)) by assuming different values of the order of reaction n. Among all these values, the plot of Y vs X will give a straight line.
- All the data obtained for the different values of n will be fitted. The n with the best fit line based on highest correlation coefficient will be considered as the correct value of reaction order.

Once the order of reaction n has been calculated, the activation energy and pre-exponential/frequency factor can be calculated as follows;

- **Activation Energy E:** The slope from the plot of parameter Y vs X (equation (2.14)) is  $s = -E/R$ , thus, the activation energy value can be obtained by the calculation of the slope from the graph.
- **Pre-exponential Factor A:** Based on equation (2.14), pre-exponential factor can be obtained from the intercept of straight line with the vertical axis. The interception between the straight line which corresponds to the chosen order of reaction and the vertical axis takes place at the following value of Y parameter:

$$Y_{interception} = \ln\left(\frac{A}{\beta}\right) \quad (3.2)$$

Thus, once the value of the interception point is obtained from the graph, the pre-exponential factor can be calculated by substituting the known parameters into equation (3.2)

#### Coats and Redfern

- **Determining the order of reaction, n**

- **When  $n \neq 1$**

- Plotting the parameters Y and X from equation (2.18) and (2.19), the order of reaction n, can be obtained as follows:
- Y parameter defined by equation (2.18) would be analyzed alongside values of parameter X (equation (2.19)) by assuming different values of the order of reaction n. Among all these values, the plot of Y vs X will give a straight line.
- All the data obtained for the different values of n will be fitted. The n with the best fit line based on highest correlation coefficient will be considered as the correct value of reaction order.

- **When  $n = 1$**

- Determination of order of reaction is skipped because n value has been assumed. Parameters Y and X is plotted from equation (2.20) and (2.21) which gives a straight line.

Once the order of reaction  $n$  for case ( $n \neq 1$ ) has been calculated, the activation energy and pre-exponential/frequency factor can be calculated for both cases as follows;

- **Activation Energy E:** The slope from the plot of parameter Y vs X (equation (2.22)) is  $s - E/R$ , thus, the activation energy value can be obtained by the calculation of the slope from the graph.
- **Pre-exponential Factor A:** Based on equation (2.22), pre-exponential factor can be obtained from the intercept of straight line with the vertical axis. The interception between the straight line which corresponds to the chosen order of reaction and the vertical axis takes place at the following value of Y parameter:

$$Y_{interception} = \ln\left(\frac{AR}{\beta E}\right) \quad (3.3)$$

Thus, once the value of the interception point is obtained from the graph, the pre-exponential factor can be calculated by substituting the known parameters into equation (3.3)

### Horowitz and Metzger

- **Determining the Activation Energy**  
Based on equation (2.31), the plot of  $\ln(\ln(W_0/W))$  against  $\theta$  gives a straight line with a slope of  $E_a/RT_s^2$ . From the thermogravimetric curves of polymer degradation and the application of the method of Horowitz and Metzger, the activation energy of degradation was established for each experiment.
- **Pre-exponential Factor A:** The corresponding value of pre-exponential factor can be calculated from equation (3.4)

$$-1 = \frac{A RT_s^2}{\beta E_a} = \exp\left(-\frac{E_a}{RT_s}\right) \quad (3.4)$$

### 3.3 Kinetics Modelling

Once the results from thermogravimetric analysis was obtained, it was used in computing an algorithm that reproduced similar result with the experimental results from thermogravimetric analysis. This algorithm was coded using Math Lab, all code was generated using the equations below and can be seen in Annex. Fig (3-4) below summarizes the experimental procedure and the modelling process.

#### 3.3.1 Development of Kinetic Model

(Scott, 2006) related the function of activation energy and time which can be expressed as:

$$M_{V(t)} = \int_0^\infty m(E, t) dE \quad (3.5)$$

Where

- $M_V(t)$  is the total mass of volatile matter

By assuming first order reaction, equation (3.5) is reduced to:

$$m(E, t) = m_o(E) e^{-A(E) \int_0^t e^{\left(\frac{-E}{RT}\right)} dt} \quad (3.6)$$

Where

- $m_o(E)$  is the initial mass of volatile matter decomposing with activation energy within the interval of  $E$  to  $E+dE$

Since  $m(E,t)$  cannot be quantified but the total mass of volatile matter or the total rates of decomposition can be measured hence, by integrating over all energies, (Scott, 2006) equation (3.6) becomes:

$$\frac{M_{V(t)}}{M_{V0}} = \frac{M_{V0} - V(t)}{M_{V0}} = \int_0^\infty g(E) * \underbrace{e^{\left[-A(E) \int_0^t e^{\left(\frac{-E}{RT}\right)} dt\right]} dE}_{\Psi(E,t)} \quad (3.7)$$

Where

- $M_{V0}$  is the initial value of  $M_V(t)$ ,
- $\Psi(E,t)$  is the double exponential term
- $V(t)$  is the volatiles yield
- $g(E)$  is the distribution of activation energy

$$g(E) = \frac{M_o(E)}{\int_0^\infty m_o dE} \quad (3.8)$$

Equation (3.7), shows the complexity of the DAEM due to the double integral term. However, different researchers in literature have been able to give a close form of this double integral and thus prevented the need for numerical integration. This has made it easier for the simplification of this model.

(Scott, 2006) described the weight loss as function of time for material decomposing via several first order reaction as:

$$\frac{M(t)}{M_0} = W + \sum_{All\ reactions\ i} f_{i,0} e^{\left[-A_i \int_0^t e^{\left(\frac{-E_i}{RT(t)}\right)} dt\right]} \quad (3.9)$$

Where

- $M(t)$  is a mass of sample that contains a fraction  $w$  of inert material
- $M_0$  is the initial value of  $M$
- $f_{i,0}$  is the fraction of  $M_0$  that decomposes with an activation energy  $E_i$  and pre-exponential factor  $A_i$

From equation (3.9),  $M(t)$  was measured experimentally, the challenge is to find the unknown terms in the equation. Equation (3.9) would be a linear equation if all the reactions and kinetic parameters ( $E$  and  $A$ ) are known. The mass of a solid fuel at any given time, is the sum of the masses of each



component remaining. Hence, equation (3.9) can be rewritten as a matrix equation for any set of time  $t_1, t_2, t_3$ , and the mass of fuel remaining,  $M(t)$ , is given by:

$$\frac{1}{M_0} \begin{bmatrix} M(t_0) \\ M(t_1) \\ M(t_2) \\ \vdots \\ M(t_n) \end{bmatrix} = \underbrace{\begin{bmatrix} \Psi_1(t_0) & \Psi_2(t_0) & \dots & \Psi_z(t_0) & 1 \\ \Psi_1(t_1) & \Psi_2(t_1) & \dots & \Psi_z(t_1) & 1 \\ \Psi_1(t_2) & \Psi_2(t_2) & \dots & \Psi_z(t_2) & 1 \\ \Psi_1(t_3) & \Psi_2(t_3) & \dots & \Psi_z(t_3) & 1 \\ \vdots & \vdots & \ddots & \ddots & 1 \end{bmatrix}}_{\underline{\Psi}} * \begin{bmatrix} f_{1,0} \\ f_{2,0} \\ f_{3,0} \\ \vdots \\ \underline{f} \end{bmatrix} \quad (3.10)$$

$$\text{i.e. } \underline{M} = \underline{\Psi} * \underline{f}$$

At constant heating rate, the equation is reduced to

$$\Psi_i(t) = \Psi_i(T) = e^{\left[ \frac{-A_i}{B} \int_{T_0}^T e^{\left(\frac{-E_i}{RT(t)}\right)} dT \right]} \quad (3.11)$$

The initial mass fraction  $f_{i,0}$ , decomposing in each reaction  $i$  was calculated using the equation below based on the assumption of a continuous Gaussian Distribution of Activation Energies and a common value for the frequency factor

$$\frac{V_{\infty} - V}{V_{\infty}} = [\sigma(\sqrt{2\pi})^{-1} \{ \int_0^{\infty} \exp - ( \int_0^t k dt ) f(E) \delta E \}] \quad (3.12)$$

Equation (3.10) was solved using the least square approach with each mass fraction becoming a parameter that was used to reduce the difference between the values of  $\underline{M}$  and  $\underline{\Psi} * \underline{f}$  which was subjected to the constraint of only positive values.

To solve equation (3.10) using assumed values of  $A$  and  $E$ , a set of reaction is generated. After this, matrix can be calculated. The assumption is that for any conversion, there is a single reaction dominating. Thus, the fraction of the initial mass remaining at constant heating rate is given by the equation below.

$$f_i(T) = f_{i,0} e^{\left[ -A_i \int_0^t e^{\left(\frac{-E_i}{RT}\right)} dT \right]} = f_{i,0} \Psi_i(T) \quad (3.13)$$

The activation energy for this study was calculated using the equation below (Scott, 2006)

$$\frac{1}{B_1} \left[ T_0 e^{\left(\frac{-E_i}{RT_0}\right)} - \frac{E_i}{R} \int_{\frac{E}{RT_0}}^{\infty} \frac{e^{-u}}{u} du - T_1 e^{\left(\frac{-E_i}{RT_1}\right)} + \frac{E_i}{R} \int_{\frac{E}{RT_1}}^{\infty} du \right] = \frac{1}{B_2} \left[ T_0 e^{\left(\frac{-E_i}{RT_0}\right)} - \frac{E_i}{R} \int_{\frac{E}{RT_0}}^{\infty} \frac{e^{-u}}{u} du - T_2 e^{\left(\frac{-E_i}{RT_2}\right)} + \frac{E_i}{R} \int_{\frac{E}{RT_2}}^{\infty} \frac{e^{-u}}{u} du \right] \quad (3.14)$$

After determination of the activation energy  $E_i$ , to obtain the pre-exponential factor,  $A_i$ , the value below can be used based on the assumption that the dominating reaction is at some conversion. The conversion refers to individual component and not overall conversion of mass of plastics to volatile material.

$$X = 1 - \frac{1}{e} \Rightarrow \Psi_i = \frac{1}{e} \approx 0.368 \quad (3.15)$$

Thus, for this study the pre-exponential factor,  $A_i$ , was calculated using the equation below (Scott, 2006)

$$\ln(\Psi_i) = -1 = \frac{A_i}{B_1} \left[ T_o e^{\left(\frac{-E_i}{RT_o}\right)} - \frac{E_i}{R} \int_{\frac{E}{RT_o}}^{\infty} \frac{e^{-u}}{u} du - T_2 e^{\left(\frac{-E_i}{RT_2}\right)} + \frac{E_i}{R} \int_{\frac{E}{RT_2}}^{\infty} \frac{e^{-u}}{u} du \right] \quad (3.16)$$

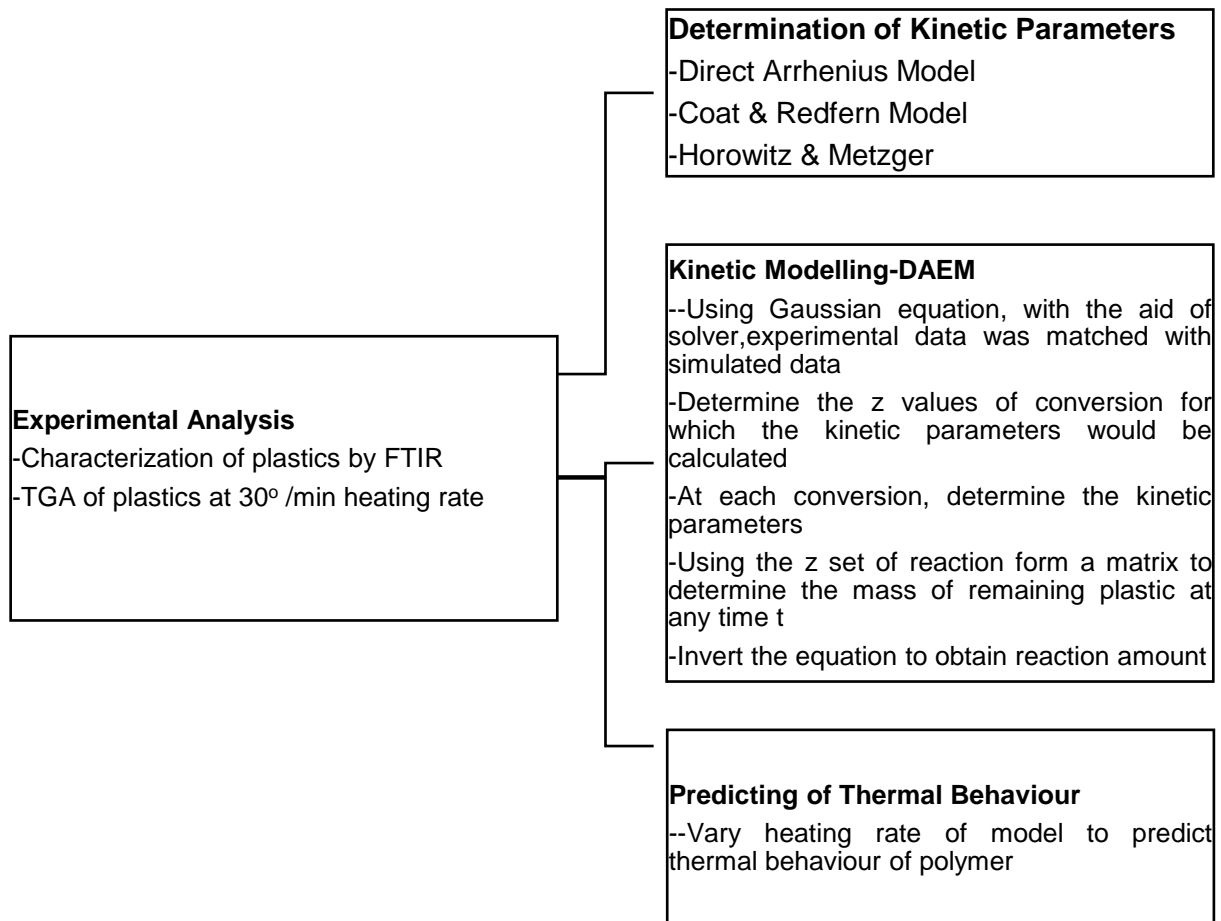


Figure 3-4 Work Flow of Experimental and Modelling Process

## 4 Results and Discussion

### 4.1 Plastic Characterization

#### 4.1.1 Fourier Transform Infrared Spectroscopy (FTIR)

A minimum of four absorption is required for characterization based on Table 3-1. The IR spectra for the municipal solid plastic waste is shown graphically from (Fig. 4-1) to (Fig.4-7) below. Based on this analysis, plastics was grouped based on its polymer type as presented in Table 4-1

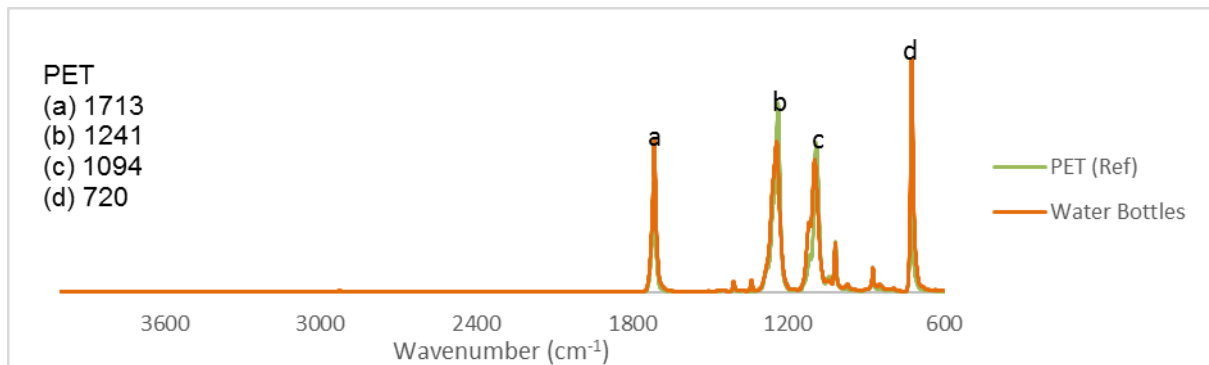


Figure 4-1 FTIR Spectra of PET

From Fig (4-1), the FTIR spectrum of PET displays that the peak exhibited at  $1713\text{ cm}^{-1}$  is attributed to the stretching of C=O of carboxylic acid group. Two peaks were also observed at  $1241$  and  $1094\text{ cm}^{-1}$ , which corresponds to vibrations of the ester C-O bond. Peak at  $720\text{ cm}^{-1}$  represents the interaction of polar ester groups and benzene rings.

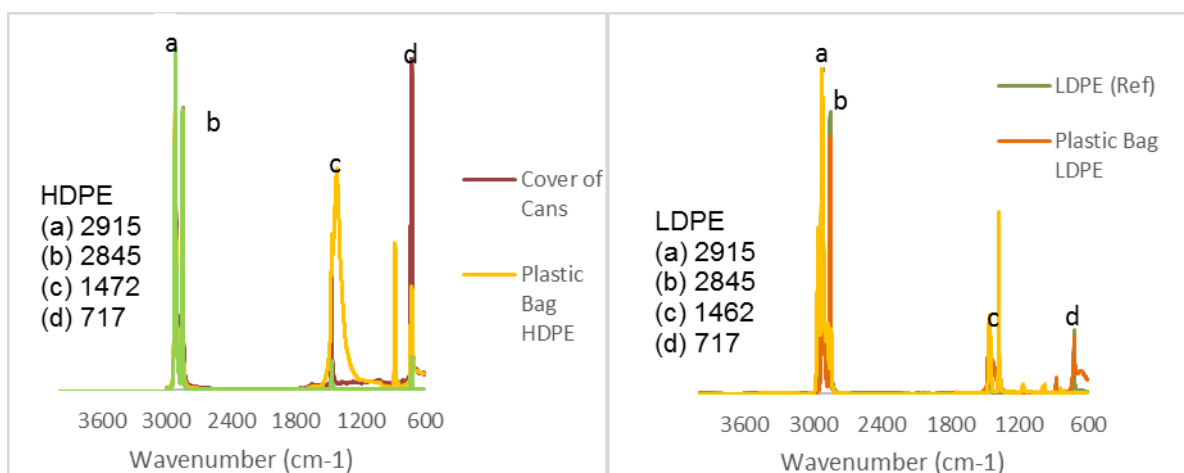


Figure 4-2 FTIR Spectra of HDPE

Figure 4-3 FTIR Spectra of LDPE

Fig (4-2) and Fig (4-3) shows the IR spectra for HDPE and LDPE which shows the similarities of both polymers however peaks(point c & d) are not identical in shape, reflecting the fact at those frequencies, the materials do not absorb IR radiation identically, and so do not have exactly the same structure. Two peaks were also observed at  $2915$  and  $2845\text{ cm}^{-1}$  for both polymers, corresponds to stretching of the C-H bond. While the other peaks at  $(1472\text{ \& } 717\text{ cm}^{-1})$  and  $(1462\text{ and } 717\text{ cm}^{-1})$  for

HDPE and LDPE respectively, indicates CH<sub>2</sub> rocking. From both plots it can be observed that both polymers have a set of close and sharp peaks this indicates polymer crystallinity.

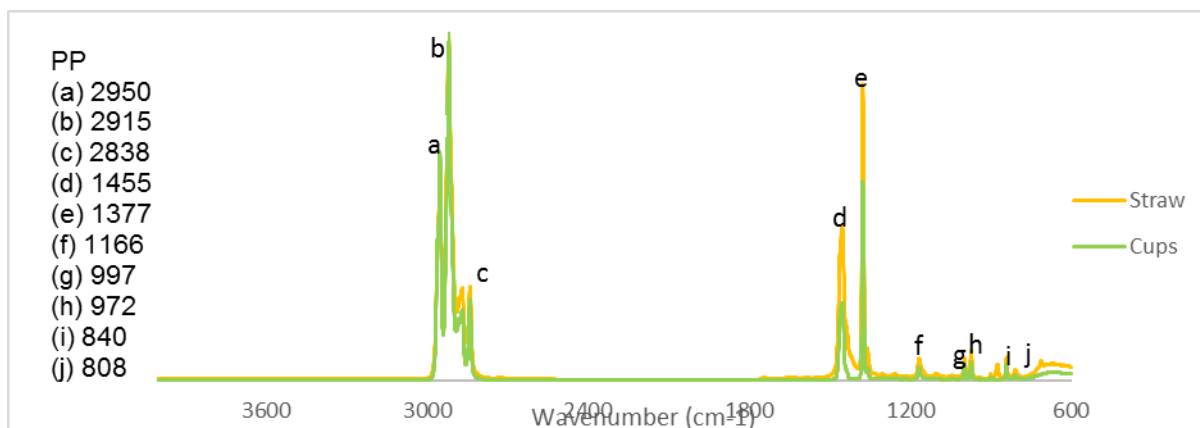


Figure 4-4 FTIR Spectra of PP

Fig (4-4) shows the IR spectra for polypropylene. No reference material was obtained however the grouping of the FTIR spectra was based on published literatures. Spectrum shows evidence of absorption bands at 2950, 2915, 2838 cm<sup>-1</sup> which indicates stretching of C-H bond, 1455 cm<sup>-1</sup> shows CH<sub>3</sub> bending, 1377 cm<sup>-1</sup> (CH<sub>3</sub> bend), 1166 cm<sup>-1</sup> (CH bend, CH<sub>3</sub> rock, C-C stretch), 997 cm<sup>-1</sup> (CH<sub>3</sub> rock, CH<sub>3</sub> bend, CH bend), 972 cm<sup>-1</sup> (CH<sub>3</sub> rock, C-C stretch), 840 cm<sup>-1</sup> (CH<sub>2</sub> rock, C-CH<sub>3</sub> stretch) and 808 cm<sup>-1</sup> (CH<sub>2</sub> rock, C-C stretch, C-CH stretch).

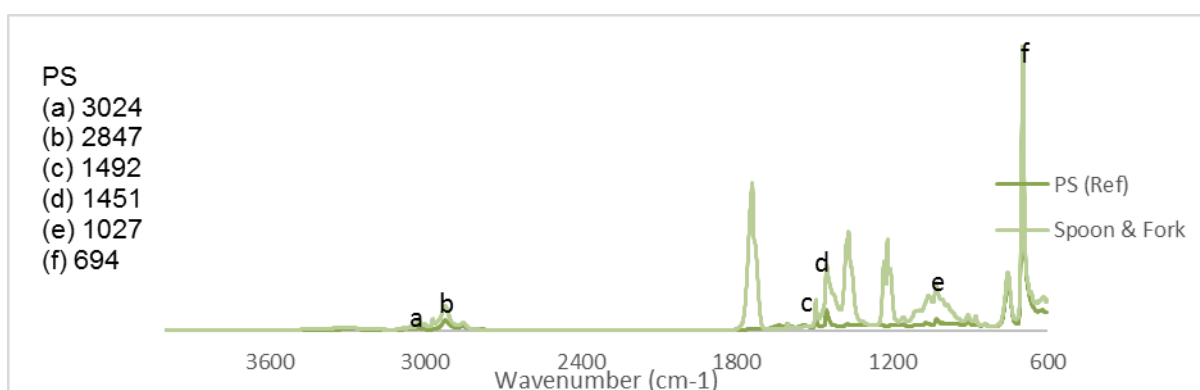


Figure 4-5 FTIR Spectra of PS

From Fig (4-5), it can be observed that the first peak is at 3024 cm<sup>-1</sup> and it indicates aromatic C-H stretching vibration. Peak at 2848 cm<sup>-1</sup> corresponds to C-H asymmetric and symmetric stretching band. Peak at 1492 cm<sup>-1</sup> corresponds to aromatic ring stretch. Peak at 1451 cm<sup>-1</sup> are corresponds to CH<sub>2</sub> bending deformation. 1027 and 694 cm<sup>-1</sup> peaks corresponds to aromatic C-H deformation vibration.

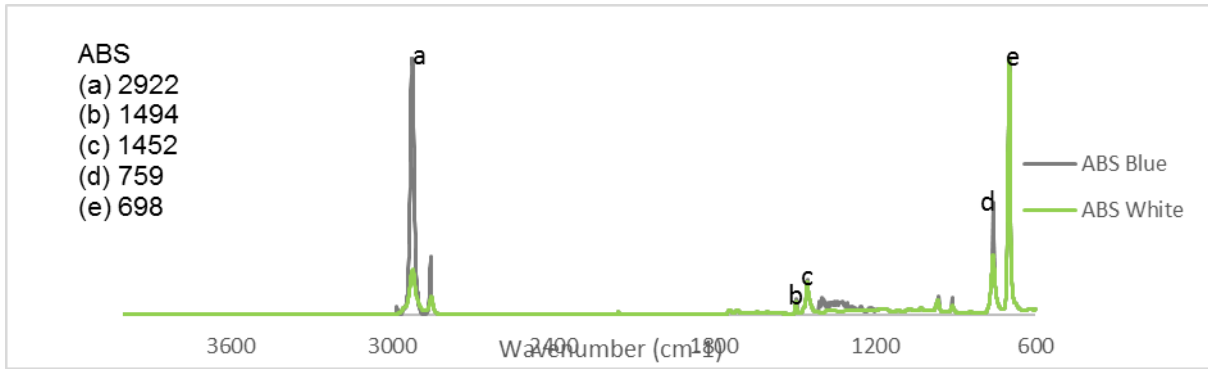


Figure 4-6 FTIR Spectra of ABS

From Fig (4-6), peak at  $2922\text{cm}^{-1}$  corresponds to C-H stretching,  $1494\text{ cm}^{-1}$  indicates aromatic ring stretching while peaks  $1452\text{ cm}^{-1}$ ,  $759\text{ cm}^{-1}$  and  $698\text{ cm}^{-1}$  indicates  $\text{CH}_2$ , =CH bend and aromatic CH out of plane bend respectively.

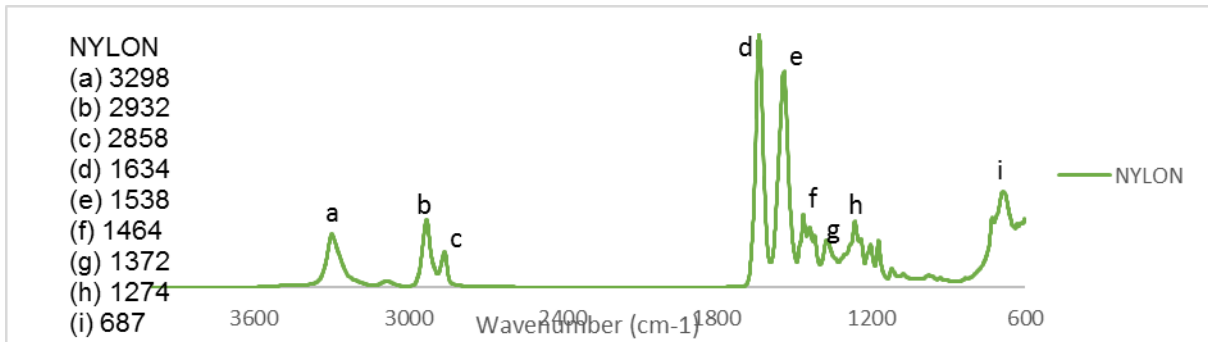


Figure 4-7 FTIR Spectra of NYLON

From IR spectra of NYLON (Fig 4-7), spectrum shows absorbance at  $3298\text{cm}^{-1}$  (N-H stretch),  $2932\text{cm}^{-1}$  (CH stretch),  $2858\text{cm}^{-1}$  (CH stretch),  $1634\text{cm}^{-1}$  (C=O stretch),  $1538\text{cm}^{-1}$  (NH bend, C-N stretch),  $1464\text{cm}^{-1}$  ( $\text{CH}_2$  bend),  $1372\text{cm}^{-1}$  ( $\text{CH}_2$  bend),  $1274\text{ cm}^{-1}$  (NH bend, C-N stretch) and  $687\text{ cm}^{-1}$  (NH bend, C=O bend).

Comparison of the reference material with waste polymer IR spectra indicates the presence of same functional group however, the respective peaks are of slightly different proportions. The reason for this can be attributed to the fact that some waste polymer like plastic bags (Fig 4.2) during the manufacturing process, color additives was included, and this is the reason why some peaks are fatter than the established reference.

Table 4-1: Grouped Municipal Solid Plastic Waste

Polymer Type	Municipal Solid Plastic Waste
PET	Water bottles, Coca-Cola bottles
HDPE	Cover of cans, plastic bags, Facial wipes
LDPE	Plastic bags
PP	Straws, Cups
PS	Spoon, Fork
ABS	Reference material
NYLON	Reference material

### 4.1.2 Thermogravimetry Analysis

The weight loss curve (TG) (Fig. 4-8) shows the loss of mass with temperature at 30°C/min heating rate for all plastics types used in this study. The plot shows that all plastic type exhibit similar temperature behavior and have same shape of the decomposition curves. TGA curves can be broken down into three parts. First part shows dehydration (moisture evaporation), second part shows the maximum devolatilization which is the active stage and the third part is continuous slight devolatilization which usually have higher percentage of solid residue. The DTG curve (Fig 4-9) is the first derivation of the TG curve and it shows the mass change per time along the temperature program.

For all plastic waste in this analysis, the maximum degradation was achieved within 450–520°C (Fig 4.8) with single step decomposition. Single step decomposition indicates the presence of carbon-carbon bond that promotes the random scission mechanism with an increase in temperature (Miandad, 2019).

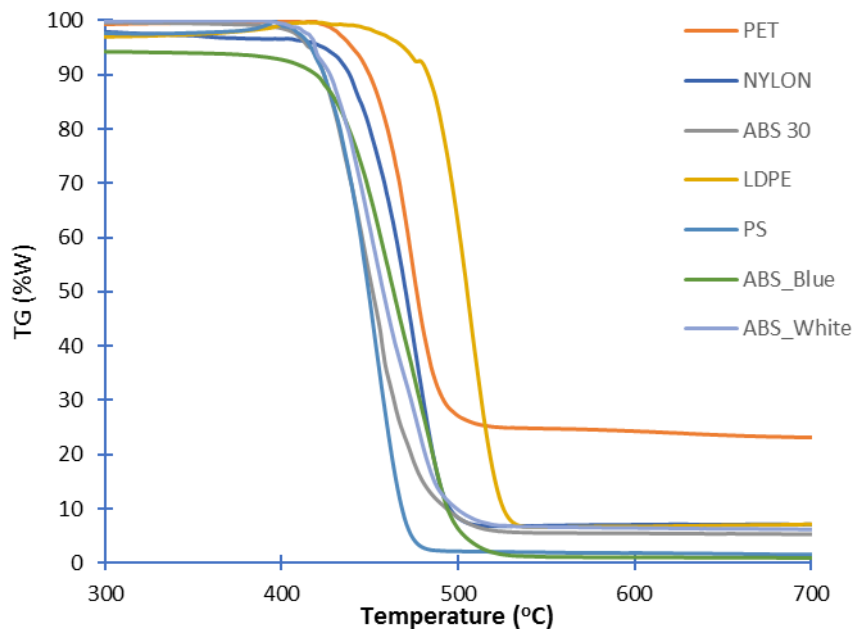


Figure 4-8 Thermogravimetric Analysis (TGA) of Plastic Waste

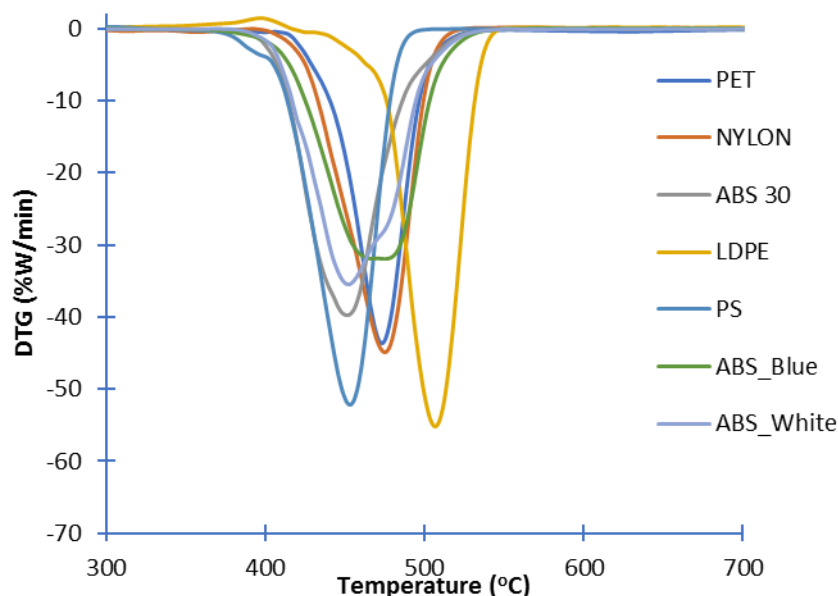


Figure 4-9 Derivative thermogravimetry (DTG) of Plastic Waste

PS has a cyclic structure, and its maximum weight loss degradation under the thermal condition involves both random chain and end-chain scission which enhances the process (Miandad, 2019). The initial decomposition started at 370 °C and reached its maximum decomposition point of 98.4% at 700°C (Fig.4-8). From literature, it can be observed that PS fully decomposes which agrees with this study however, slight variation may be due additives added in the preparation of the polymer. The optimum temperature for conversion of PS plastic waste into liquid via pyrolysis is 480°C this is because additional increase of temperature from 500 to 700°C resulted in 0.6% weight loss. Similar phenomenon can be observed in the DTG curve (Fig.4-9) where an endothermic peak is attributed to the decomposition of PS plastic. The onset melting temperature is around 370°C, melting peak around 454 °C and melting offset around 500 °C. Miandad, Rashid & Nizami, carried out a thermogravimetric analysis on PS with an onset temperature of 330°C and maximum degradation was at 470°C (Miandad, 2019). Jeffery D. Peterson, Sergey Vyazovkin, Charles A. Wight also studied the kinetic thermal degradation on PS, it degrades in a single step reaction with onset temperature at 250°C and ending at 500°C (JefferyD.Peterson, 2001) Thus, the result obtained from this study is in agreement with the results from published data.

Fig4-8 shows PET starts to decompose at around 400°C, although previous studies reported that PET starts to decompose at temperatures varying from 190, 252 and 400°C which is dependent on the polymer grade and experimental set-up (Miandad, 2019) (Lettieri, 2001) In PET thermal degradation process, the initial step is the scission of the chain of the ester linkage either through random scission at the ester linkages or through chain ends leading to a reduction in molecular weight and an increase in carboxyl end-groups (S. Venkatachalam, 2012) At 500°C the sample has lost 65.6% of its initial weight. The maximum degradation for PET was 70%. Saha and Ghoshal (Saha, 2005) studied the

pyrolysis kinetics of two PET samples under non-isothermal conditions and it was reported that both samples exhibited 70-80% weight loss between 380-515°C; this was attributed to the slower heating rates used in their study (10, 15 and 25°C min<sup>-1</sup>). The DTG indicates a single step reaction with melting peak at 474°C. The optimum temperature for pyrolysis is 474°C.

For all ABS, decomposition occurs within 370-520°C. However, slight variation was observed for the different polymer regarding the maximum decomposition at 700°C. ABS\_Blue achieved its maximum decomposition point of 98.8%, ABS\_White 92% and ABS 30 at 93% (Fig. 4-8). Additional increase in temperature from 520°C up to 700 °C showed less than 1% sample weight loss, completing the degradation of plastic with some residue leftover. For all ABS polymer, optimum pyrolysis temperature is 500°C. DTG curve (Fig. 4-9) shows the melting temperature peaks for the ABS\_White, ABS\_Blue and ABS 30 as 454,474 and 452 respectively. Similar results was obtained for thermal degradation ABS resin1 by Hitachi High Tech (Hitachi High Tech. Science Coporation, 1995). From the study, polymer decompose between 350°C and 500°C by single step process with its melting peak temperature at 435.7 °C.

NYLON from (Fig. 4-8) starts initial decomposition at 400°C, although previous studies indicates that Nylon starts to decompose at 350°C. Another study by Shodhanga on the TGA of NYLON, from the studies, it was observed that nylon exhibited single-stage degradation and a sharp weight loss occurs in the range of 398-478°C with DTG peak at 440°C (Shodhganga, Thermal Stability and Degradation Kinetics, 2012).At 500°C, the sample has lost 90% of its initial weight. The maximum degradation for PET was 91% at 700°C. The DTG indicates a single step reaction with melting peak at 477°C. The optimum temperature for conversion of NYLON plastic waste into liquid via pyrolysis is 477°C.

The thermal degradation of LDPE as shown in Fig (4-8) shows a single-stage degradation and the sharp weight loss occurring within the range of 350-550°C with the DTG peak at 507°C. At 550°C, the sample has lost 92% of its weight. Within temperature range of 50-350°C, an initial weight loss of 1-5% occurs which may be due to the removal of absorbed moisture as observed from the TGA plot. Result from this study agrees with literature study (Shodhganga, Thermal Stability and Degradation Kinetic, 2012)

## **4.2 Determination of Kinetic Parameters**

### **4.2.1 Graphical Method**

Graphical model which includes Coats & Redfern and Direct Arrhenius, both uses the Arrhenius expression to correlate the rate of mass loss with temperature. Table 4-2 and Table 4-3 shows the kinetic parameters for the different plastics obtained at 30°C/min heating rates for these models. It can be observed that kinetic parameters computed at same heating rate for these models, shows similar results as presented in Table 4-4. (Fig 4-10) to Fig (4-16) shows the order of reaction chosen for plot approach based on the R<sup>2</sup> value.



Table 4-2: Kinetic Parameters Obtained by Direct Arrhenius Model

Plastic Polymer	Reaction Order	Activation Energy, E (kJ/mol)	Frequency Factor A (sec <sup>-1</sup> )	R <sup>2</sup>
ABS_White	0.2	212	2.92E+17	0.74
	0.3	209	2.77E+17	0.74
	0.4	249	4.63E+20	0.51
	0.5	250	5.92E+20	0.52
	1	219	1.52E+18	0.76
ABS_Blue	0.2	240	1.50E+20	0.99
	0.3	241	1.77E+20	0.99
	0.4	242	2.08E+20	0.99
	0.5	243	2.44E+20	0.99
	1	248	5.49E+20	0.99
PS	0.2	189	1.57E+16	0.90
	0.3	193	2.47E+17	0.91
	0.4	197	3.24E+17	0.91
	0.5	202	1.39E+18	0.92
	1	222	5.26E+18	0.93
LDPE	0.2	193	1.33E+14	0.75
	0.3	202	2.97E+15	0.77
	0.4	210	5.93E+15	0.78
	0.5	218	2.65E+16	0.80
	1	260	4.64E+20	0.86
NYLON	0.2	141	1.35E+12	0.95
	0.3	147	2.37E+12	0.95
	0.4	152	3.63E+14	0.96
	0.5	157	3.80E+14	0.96
	1	175	4.16E+14	0.99
PET	0.2	283	1.16E+23	0.95
	0.3	285	1.85E+23	0.96
	0.4	288	1.09E+23	0.96
	0.5	291	1.74E+23	0.96
	1	304	4.96E+24	0.96
ABS (30)	0.2	145	5.94E+12	0.88
	0.3	151	1.57E+13	0.88
	0.4	160	4.17E+13	0.89
	0.5	161	4.21E+13	0.90
	1	188	1.43E+15	0.93

Table 4-3: Parameters Obtained by Coat &amp; Redfern Model

Plastic Polymer	Reaction Order	Activation Energy, E (kJ/mol)	Frequency Factor, A (sec <sup>-1</sup> )	R <sup>2</sup>
ABS_White	0.3	222	3.90E+16	0.99
	0.5	234	1.80E+17	0.99
	0.67	224	5.60E+16	0.99
	1	226	8.10E+16	0.99
ABS_Blue	0.3	177	6.40E+10	0.97
	0.5	189	3.00E+12	0.98
	0.67	178	8.20E+10	0.97
	1	180	1.10E+11	0.97
PS	0.3	269	4.80E+18	0.98
	0.5	284	3.40E+20	0.98
	0.67	275	1.40E+19	0.98
	1	282	4.20E+19	0.98
LDPE	0.3	275	9.81E+16	0.99
	0.5	293	1.19E+19	0.99
	0.67	286	6.43E+17	0.99
	1	298	4.96E+18	0.98
NYLON	0.3	180	8.90E+15	1.00
	0.5	188	5.80E+17	1.00
	0.67	186	4.90E+17	1.00
	1	193	4.70E+18	0.99
PET	0.3	306	1.30E+20	0.96
	0.5	328	2.97E+22	0.97
	0.67	326	3.58E+21	0.97
	1	347	1.50E+23	0.98
ABS (30)	0.3	182	1.38E+15	0.90
	0.5	203	3.45E+17	0.92
	0.67	202	3.22E+17	0.93
	1	224	4.86E+19	0.95

#### 4.2.2 Horowitz and Metzger

From the thermogravimetric curves of polymer degradation (Fig.4-8), it can be observed that the degradation process was a single step hence only one value for the activation energy of decomposition was calculated. From the plot of  $\ln \ln W_0/W$  against  $\theta$  from the Horowitz and Metzger method of analysis of the thermogravimetric curves as seen in (Fig4-10) to (Fig 4-16) and Table4-4, shows that all R<sup>2</sup> values for the equation of the lines used in activation energy calculation for all plastics were to some extent close to 1. R<sup>2</sup> values ranges from 0 to1 and these values are good indicator of how close the trendline is to actual experimental data. Thus, R<sup>2</sup> = 1 is the most reliable best fit line. From the results obtained using Horowitz and Metzger R<sup>2</sup> higher than 0.99 gives

confidence regarding the accuracy of the parameters obtained. However, Horowitz and Metzger model used in thermogravimetric analysis assumes that all products from the polymer degradation were gaseous and escaped immediately. This assumption made this model simple, but it is not realistic. Taking that into consideration, there is a possibility that the decomposition rate for this model are higher; thus, the activation energy obtained by this model might be lower as compared to the results from literature.

Table 4-4: Kinetic Parameters Obtained by Horowitz And Metzger Model

Plastic Polymer	Reference Temperature (°C)	Activation Energy (kJ/mol)	R <sup>2</sup>
ABS_White	452	138	0.99
ABS_Blue	477	151	1.00
ABS (30)	456	135	0.99
PS	454	142	1.00
LDPE	507	184	0.96
NYLON	477	167	0.98
PET	474	168	0.97

#### 4.2.3 Comparison of Kinetic Parameters

Fig 4-10 to Fig 4-16, shows the plot of the different models used to obtain the kinetic parameters in this study. Table 4-5 shows comparison of activation energy between the different models and known result based on literatures. Variation in the results obtained, could stem from the way in which the integral method have been derived. Graphical methods equations were developed by assuming kinetic parameters from Arrhenius equation, is determined by a form of  $g(X)$ , which is usually assumed.  $X$ , which is a function of both temperature and conversion, and it varies simultaneously with time. Hence, the model cannot distinguish separately temperature dependence of rate constant and the conversion. As a result of this, any model assumed can be easily fit with the experimental data not taking into consideration the variation between assumed model and the true unknown model. Force fitting of the experimental data to the hypothetical reaction can lead to obtaining ambiguous values of Arrhenius parameters.

Also, for the graphical approach model, different authors have established that this model predicts kinetic parameters quite well for a single first order reaction. However, the model tends to be inadequate in describing complex fuels. Coat & Redfern model may be inadequate in providing the proper description for non-isothermal pyrolysis because the kinetic parameters depend on specific polymer used in the experiment and order of reaction this limits the model.

Another reason for variation of kinetic parameters is the possibility of multi-reaction mechanisms with different activation energies as each step, this is influenced by temperature and extent of conversion. Thus, activation energy obtained is a function of  $T$  and  $X$ . From the results obtained, the calculated

value of activation energy, represents the average value for the overall degradation process. The value was obtained based on the assumption that these kinetic parameters do not change with reaction mechanism. However, kinetics changes as temperature change so an average kinetic parameter, is not a true representation hence the reason for the distributed activation energy model.

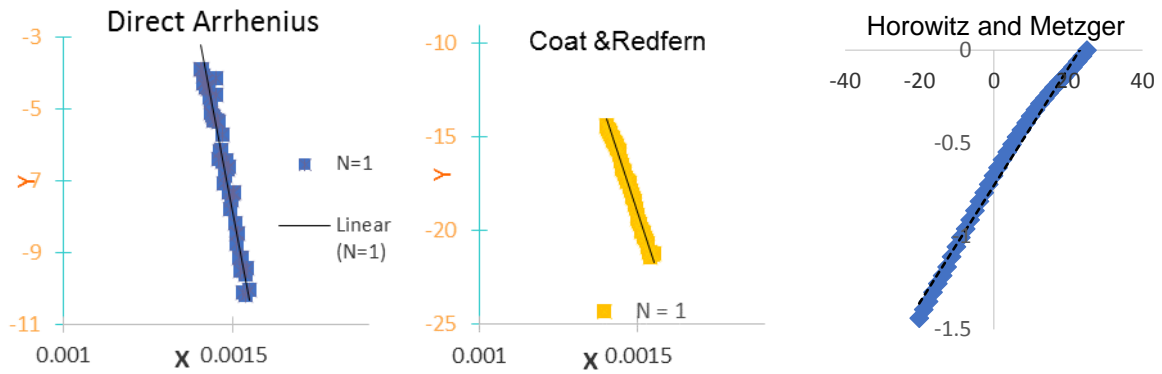


Figure 4-10 Kinetics Models Plots for ABS\_White

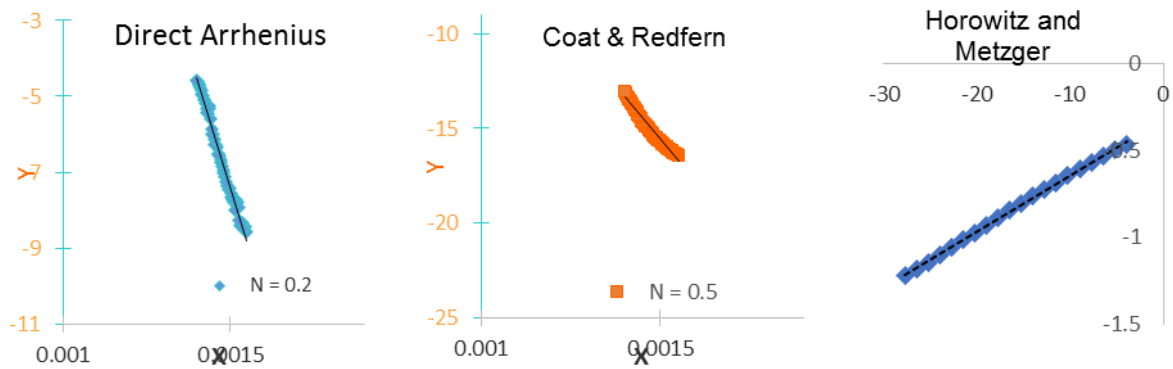


Figure 4-11 Kinetic Models Plots for ABS\_Blue

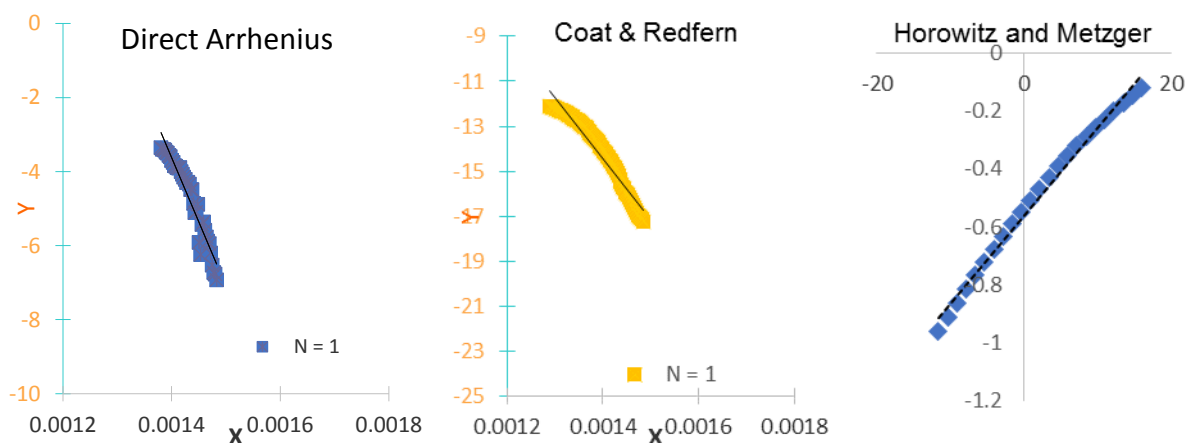


Figure 4-12 Kinetic Models Plots for ABS (30)

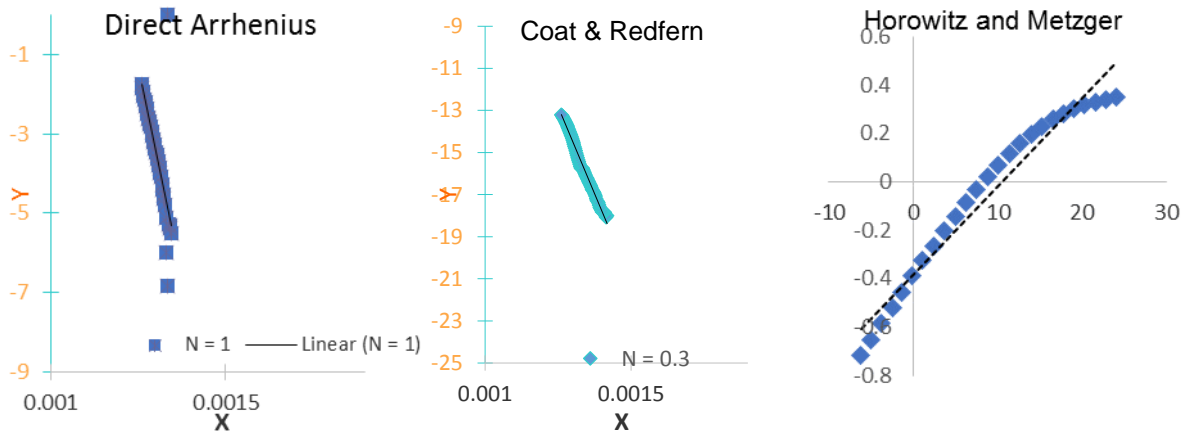


Figure 4-13 Kinetic Models Plots for LDPE

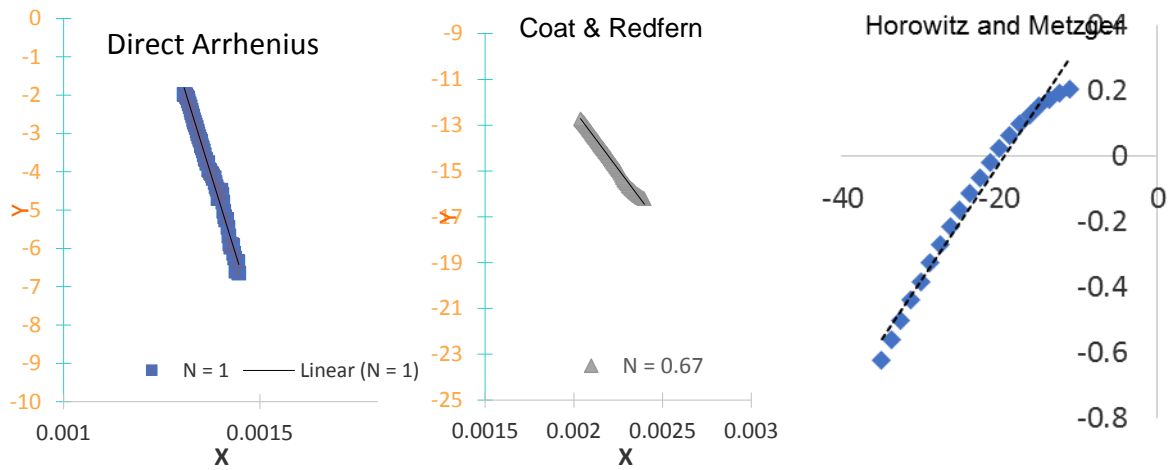


Figure 4-14 Kinetic Models Plots for NYLON

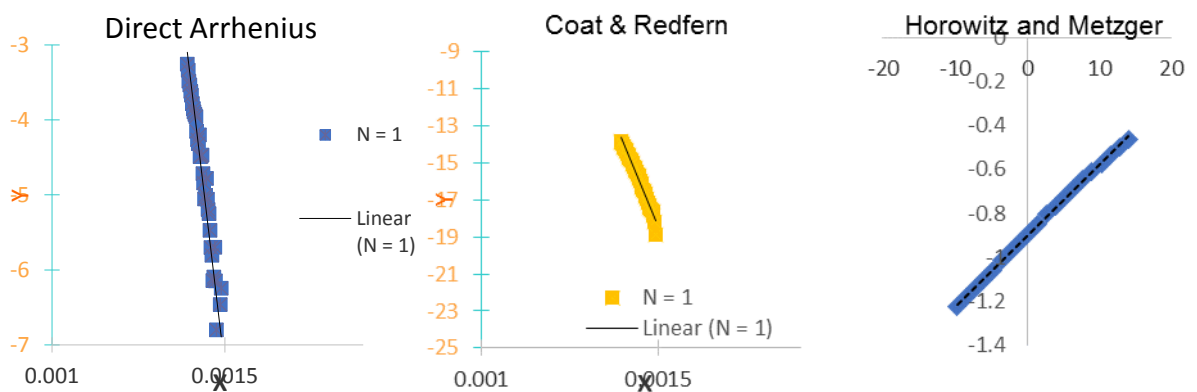


Figure 4-15 Kinetic Models Plots for PS

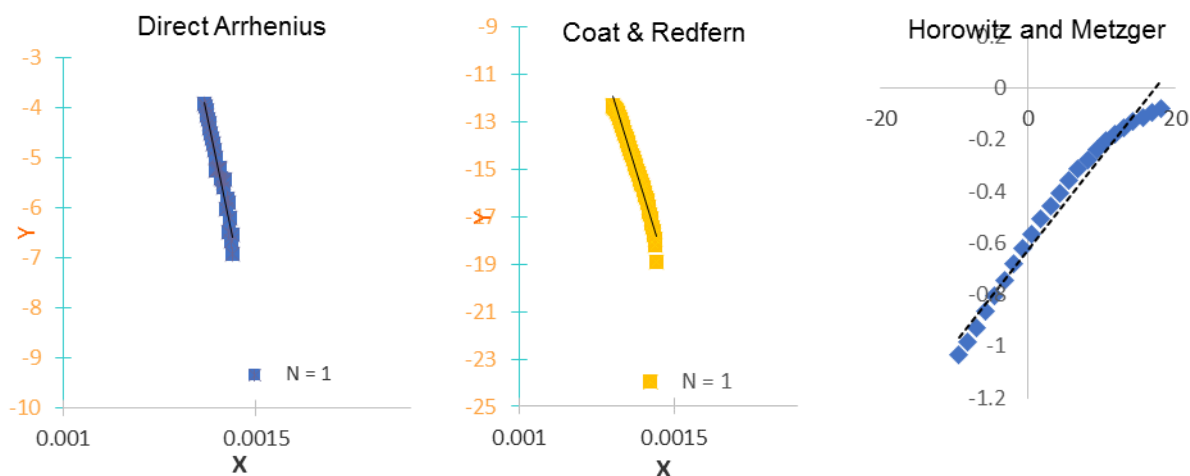


Figure 4-16 Kinetic Models Plots for PET

Table 4-5: Comparison of Activation energies

Plastic Polymer	Activation Energy (kJ/mol)			
	Direct Arrhenius	Coat & Redfern	Horowitz and Metzger	Published Data
ABS_White	219	226	138	163.3-248.95
ABS_Blue	240	189	151	163.3-248.95
ABS (30)	188	224	135	163.3-248.95
PS	222	282	142	158.15-200
LDPE	260	275	184	192- 247
NYLON	175	186	167	80-190
PET	304	347	168	180-241

R. S. Lehrle, W. Parsons, M. Rollinson in their study on the Kinetics and Mechanisms of the Thermal Degradation of Nylon 6, discovered that pyrolysis occurred in two degradation stages which is different from this study whereby degradation occurs in a single step. The reason for this variation could be due to differences in structure or chemical composition of plastic. The activation energies obtained for the first and second stage was  $170 \pm 20$  kJ/mol and  $100 \pm 20$  kJ/mol respectively which is within the range of activation energy obtained by this study using Coat & Redfern, Direct Arrhenius and Horowitz and Metzger approach. (Rollinson, 1999). Another study on the Kinetics and Thermodynamic Studies of Depolymerization of Nylon Waste by Hydrolysis Reaction by D. B. Patil and S. V. Madhamshettiwar calculated the Activation energy as 101.59 kJ/mol (Madhamshettiwar, 2014).

Rafael Balart, David Garcia-Sanoguera, Luis Quiles-Carrillo, Nestor Montanes, and Sergio Torres-Giner carried out an in-depth study kinetic study of the thermal degradation of recycled acrylonitrile-butadiene-styrene (ABS) polymer (Rafael Balart, 2019). Non-isothermal thermogravimetric analysis (TGA) for the study was done in Nitrogen atmosphere with heating rate of  $30 \text{ K min}^{-1}$ . The activation

energy obtained for the thermal degradation process of ABS was 163.3kJ/mol. H. Polli, L.A.M Pontes A.S. Araujo, Joana M. F. Barros, V. J. Fernandes Jr. also carried out a study on the degradation behavior and kinetic study of ABS polymer (H. Polli, 2009). From their study, the activation energy for the three different types of ABS polymer used was given as ABS\_GP ( $204.5 \pm 11.5$  kJ/mol), ABS\_HI, ( $239.0 \pm 9.8$  KJ/mol) and ABS\_HH ( $242.4 \pm 5.4$  kJ mol). Another study by Liu G, Liao Y, Ma X on the thermal behavior of vehicle plastic blends contained acrylonitrile-butadiene-styrene (ABS) in pyrolysis using TG-FTIR the activation energy calculated for the three different polymers of ABS were 186.63kJ/mol, 239.61kJ/mol and 248.95kJ/mol (Liu G, 2017) Thus, for ABS, it can be observed from literatures that the activation energy changes, based on the additive's that was added during the polymer manufacturing process.

S.M. Al-Salem and P. Lettieri studied the Kinetics of Polyethylene Terephthalate (PET) and Polystyrene (PS) and found the activation energies as 180.08 kJ/mol for PET and 158.15 kJ/mol for PS (Lettieri, 2001). Jeffery Peterson, Sergey Vyazovkin and Charles Wight computed the activation energy for PS and LDPE in their study kinetics of thermal and thermo-oxidative degradation of polystyrene, polyethylene and poly propylene (JefferyD.Peterson, 2001). Results obtained was 200KJ/mol for PS. Using Coat and Redfern method, Shodhganga determined the activation energy for LDPE and PET as 345 and 241kJ/mol respectively. Another study by Sinfrono obtained the activation energy for LDPE using Flynn–Wall–Ozawa, as 192kJ/mol, which is like the result obtained by this study using Horowitz & Metzger (Sinfrônio, 2005). Jin Woo Park, in the study Kinetic Analysis of Thermal Decomposition of Polymer Using a Dynamic Model obtained the activation energy for LDPE using differential method, integral method, parallel reaction method and dynamic method at 30°C heating rate as 209,247,227 and 196kJ/mol respectively. (Jin Woo Park, 2000)

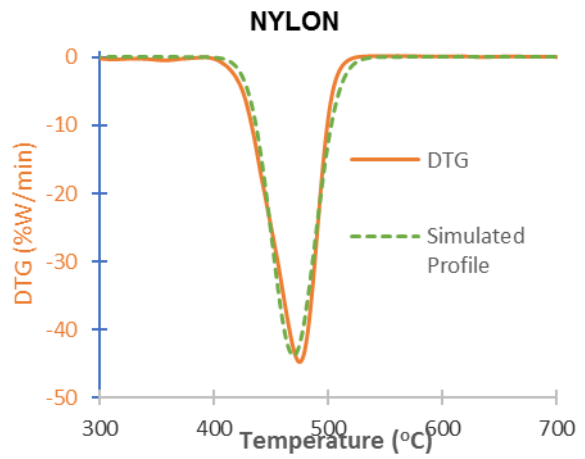
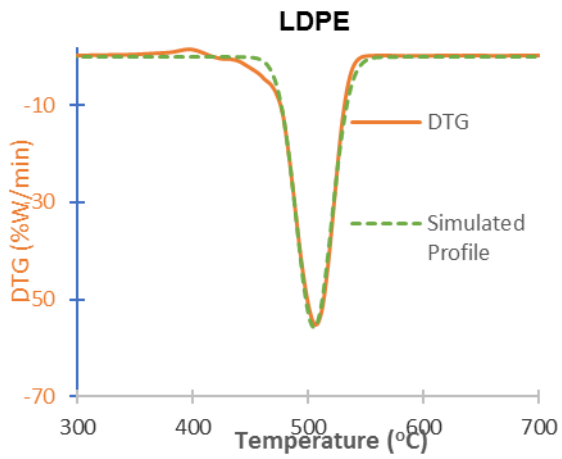
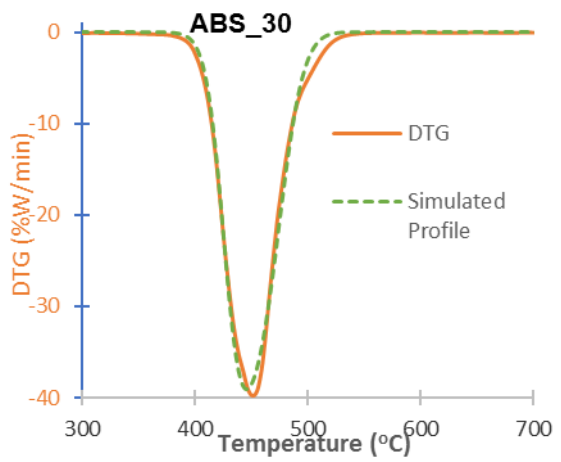
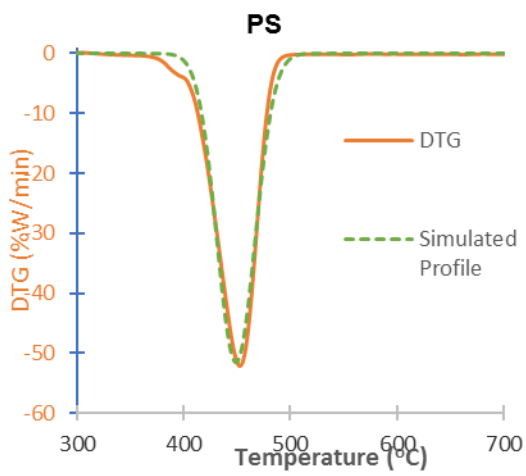
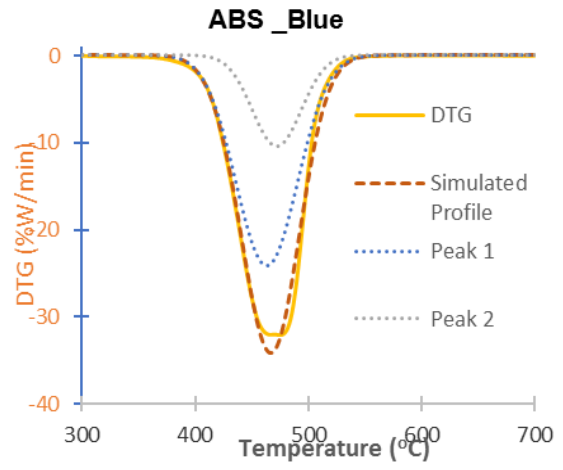
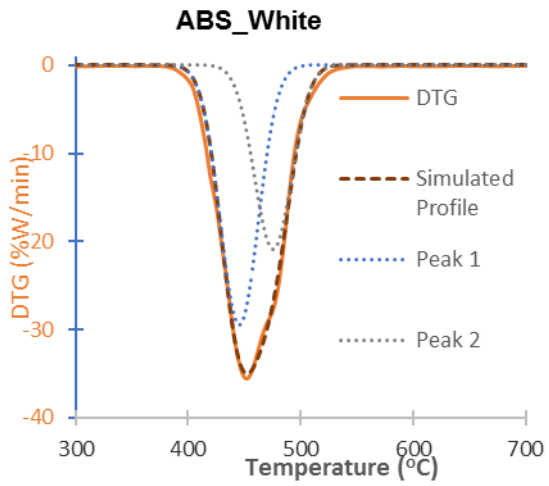
Some variations of results obtained with literature values could be due to differences in the experimental procedure for different samples (such as particle size of sample) and weighing the effects with the data analysis techniques used in the calculation of the kinetic parameters.

### **4.3 Distributed Activation Energy Model**

#### **4.3.1 Comparison of Experimental Result with Simulated Result**

The peak in DTG curve indicates a reaction taking place. So, simulation of the exact position of this peak was done using Gaussian distribution. The size of each peak for the different plastics was determined by adjusting the simulated peak temperature, peak height or intensity and peak width to fit the experimental results obtained by thermogravimetric analysis.

Solver was used in the optimization of the Gaussian distribution parameters for the different DTG profiles as shown in (Fig 4-17). From the plot, the simulated result obtained using Gaussian equation was able to replicate experimental results. However, for some plastic, some discrepancies can be observed such as overprediction or underprediction of the result. Plastics differ in structure and during manufacturing process some additives may have been added. Thus, during the degradation process, there is the possibility of reaction occurring making this process unique and different from normal distributive curve which Gaussian equation mirrors.





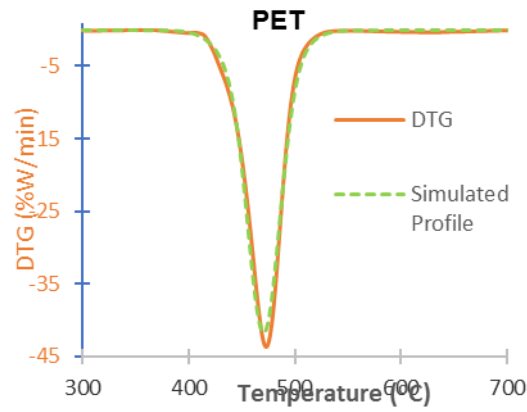


Figure 4-17 Gaussian distribution curves fitted on DTG Experimental results

### 4.3.2 Determination of Kinetic Parameters

Kinetic parameters, for the different plastics was determined using the distributed activation energy model (DAEM). This method of approach assumes that the reaction proceed through infinite number of parallel reactions each having its own activation energy. Variation in this activation energy can be shown as a continuous distribution function (Fig 4.18). Evaluation of kinetic parameters can either be by distribution free method or distribution fitting method. Gaussian distribution was used in describing the activation energy for this study.

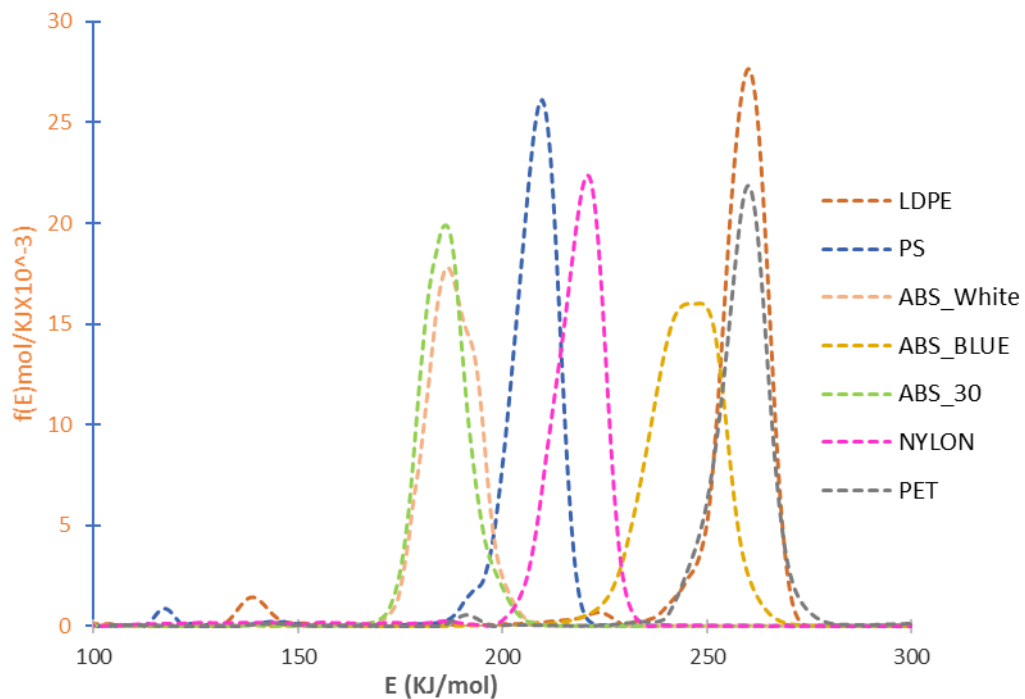


Figure 4-18 Activation Energy Distribution

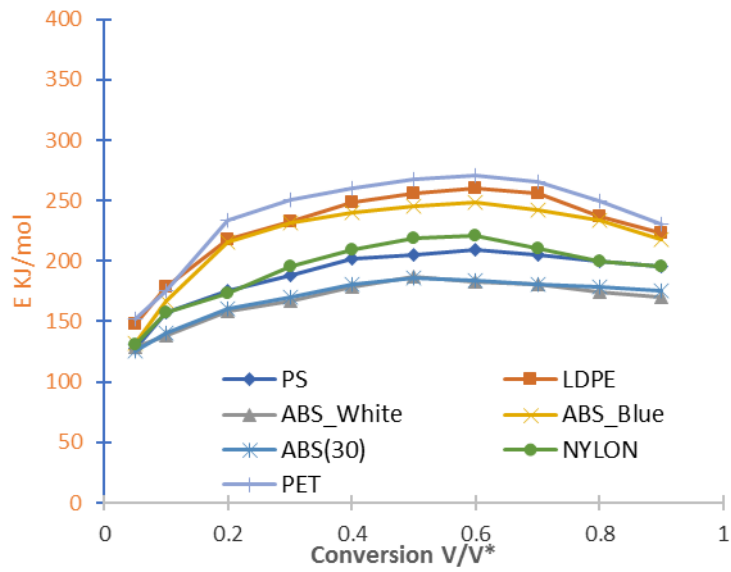


Figure 4-19 Relationship between activation energy and conversion(V/V\*)

Table 4-6: Kinetic Parameters obtained with DAEM for ABS

Conversion (V/V*)	ABS_White		ABS_Blue		ABS (30)	
	Activation Energy (kJ/mol)	Frequency Factor A (sec <sup>-1</sup> )	Activation Energy (kJ/mol)	Frequency Factor A (sec <sup>-1</sup> )	Activation Energy (kJ/mol)	Frequency Factor A (sec <sup>-1</sup> )
0.05	128.26	3.71E+10	132.46	2.74E+11	125.56	3.64E+10
0.1	138.26	2.86E+11	167.12	1.81E+13	140.38	2.90E+11
0.2	158.61	2.88E+12	215.43	6.53E+16	160.75	2.92E+12
0.3	166.65	1.74E+13	231.55	4.44E+17	170.34	1.78E+13
0.4	178.81	6.45E+14	240.55	2.74E+18	180.76	6.52E+14
0.5	186.63	1.48E+15	245.23	2.81E+18	186.13	1.48E+15
0.6	183.32	1.42E+15	248.43	2.84E+18	183.48	1.42E+15
0.7	180.67	1.37E+15	242.43	2.79E+18	180.34	1.37E+15
0.8	174.32	6.31E+14	234.23	4.47E+17	179.11	6.48E+14
0.9	170.13	6.27E+14	218.22	6.62E+12	175.23	6.46E+14
Average	166.566		217.565		168.208	

Table 4-7: Kinetic Parameters obtained with DAEM for PS, LDPE, PET and NYLON

Conversion (V/V*)	PS		LDPE		PET		NYLON	
	Activation Energy (kJ/mol)	Frequency Factor A (sec <sup>-1</sup> )	Activation Energy (kJ/mol)	Frequency Factor A (sec <sup>-1</sup> )	Activation Energy (kJ/mol)	Frequency Factor A (sec <sup>-1</sup> )	Activation Energy (kJ/mol)	Frequency Factor A (sec <sup>-1</sup> )
0.05	127.28	3.70E+10	148.19	1.38E+12	152.36	2.73E+12	130.93	2.71E+11
0.1	157.83	2.83E+12	178.30	6.69E+12	175.71	6.35E+12	157.78	2.83E+12
0.2	175.52	6.34E+14	218.00	6.61E+16	233.68	4.47E+17	172.94	6.25E+12
0.3	187.66	1.56E+15	232.62	4.45E+17	250.23	3.06E+19	195.27	1.34E+16
0.4	201.68	2.75E+16	248.87	2.85E+18	260.48	5.63E+19	208.82	4.43E+16
0.5	205.32	3.91E+16	255.65	3.13E+19	268.13	5.79E+19	218.47	6.62E+16
0.6	209.54	4.45E+16	260.18	5.62E+19	270.38	2.38E+20	220.61	1.54E+17
0.7	204.88	3.85E+16	255.66	2.66E+18	265.43	5.73E+19	210.21	4.84E+16
0.8	200.33	2.66E+16	236.72	2.87E+17	249.34	2.86E+18	200.27	2.66E+16
0.9	195.68	1.34E+16	222.82	1.18E+17	230.64	4.41E+17	195.81	1.37E+16
Average	186.570		225.700		235.638		191.111	

DAEM algorithm was run for about 100 reactions. From Table 4.6 & 4.7, shows the reactions where mass loss occur. The activation energy E obtained for ABS\_White, ABS (30) and ABS\_Blue ranged from 128.26 – 186.63, 125.56 – 186.13 and 132.46 – 248.43 kJ/mol, with average activation energy of 166.566, 168.208 and 217.565 kJ/mol respectively. However, the conversion range differ with ABS\_White and ABS (30) within the range of 0.05 – 0.5 and 0.5 – 0.9 while ABS\_ Blue within the range of 0.05 – 0.6 and 0.6 – 0.9.

Activation energy obtained for PS, LDPE, PET and NYLON ranged from 127.28 – 209.54, 148.19 – 260.18, 152.36 – 270.38 and 130.93 – 220.61 kJ/mol. Average activation energy calculated was 186.570, 225.7, 235.638 and 191.111 kJ/mol. All average results obtained using DAEM, is in accordance with literature results. Comparing the kinetic parameters obtained with Coat & Redfern, Direct Arrhenius method, it can be observed that the activation energy obtained using these methods results can be found with this continuous distribution for a particular conversion. However, DAEM was able to capture the kinetic parameters as a function of temperature.

### 4.3.3 Predicting Thermal Behavior of Plastics

Based on Gaussian distribution curve fitted on experimental data (Fig 4.17) from the best fitted plot with negligible error, kinetic behavior of ABS\_White, NYLON and PET was predicted for different heating rate.

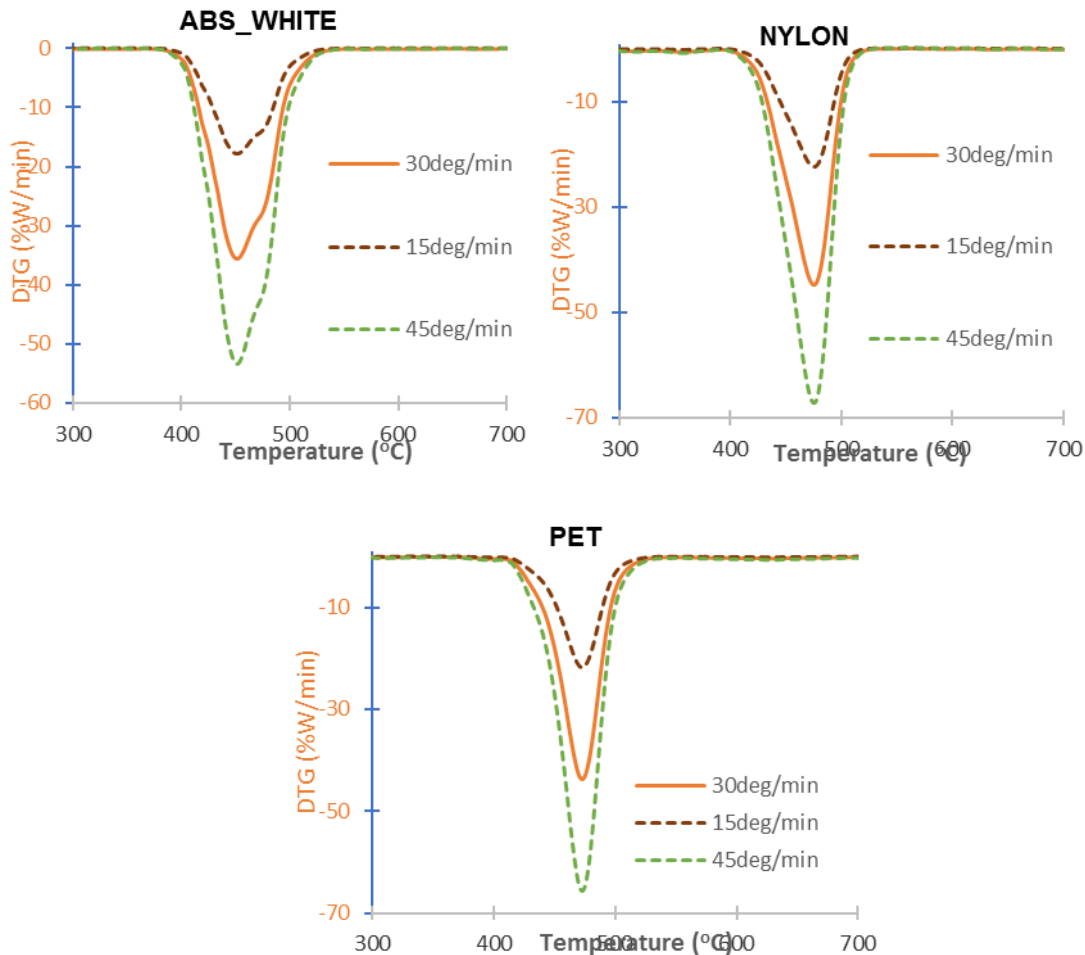


Figure 4-20 DTG prediction at different heating rate

(Fig 4.20) shows the plot of the derivative thermogravimetric analysis (DTG) for the aforementioned plastics at 15°C/min and 45°C/min heating rate in comparison to the experimental heating rate(30°C/min). From the plot, it can be observed that the shape and peak of simulated results matches the experimental results for all plastics. Heating rate affect the thermal profile of material. An increase in the heating rate, increases the initial, final temperature and the peak temperature. From the plot, it can be observed that increasing the heating rate, causes the DTG curve to become bigger and peak temperature becomes higher.

This model algorithm was made to replicate the behavior of the experimental result with heating rate of 30°C/min not factoring the possibility of secondary reactions.

## 5. Conclusions and Future Works

Plastics seems to be part of our daily lives and this contribute to approximately 10% of discarded waste and only about 25% is being recycled. Annual waste generated is expected to increase by 70% to about 3.4 billion tonnes in 2050 due to rapid increase in population and urbanization. Currently it is very difficult to find an alternative to plastic and the question is what is done after its useful life. Energy plays an important role in the life cycle of plastics. With the increasing demand for energy, the world is faced with finding the right fuel that would not deplete finite stock but also reduce environmental concerns. From the sustainability point of view, energy used in production should be recovered by at the end of the useful life of a product.

Pyrolysis of waste plastic seems to be the most suitable method in terms of economics in solving the steadily increasing growing amount of plastic waste and meeting the growing energy demand. Pyrolysis is a complex process and for this process to be done efficiently, understanding the kinetics of the reaction is vital. In this study, the different plastic waste was characterized by their absorption band using the FTIR analysis. Thermogravimetric analysis (TGA) was used in the evaluation of thermal decomposition behavior of the plastics. The maximum degradation was achieved within 450–520°C with single step decomposition which indicates the presence of carbon-carbon bond that promotes the random scission mechanism with an increase in temperature. Different models exist that can be used in the prediction of kinetic parameters based on thermogravimetric analysis and they differ based on the mathematical function used in describing them. Kinetic parameters for this study was obtained using Direct Arrhenius Method, Coat & Redfern and Horowitz and Metzger. The result obtained using these models was within the range of result obtained from published data. However, these mathematical models use unrealistic assumptions that may not be accurate in predicting the true pyrolysis behavior of the polymer, hence it cannot give a proper understanding of how pyrolysis occur and how the process can be optimized thus the reason for the distributed activation energy model (DAEM)

Distributed Activation energy model assumes that pyrolysis of complex fuel is a first order decomposition with different chemical group and each group is having its own unique activation energy for the decomposition process. Activation energy is said to follow a continuous distribution function and for this study, it was the Gaussian distribution. The DAEM algorithm was developed using MATLAB and data obtained from TGA experiments which was used in calculation of kinetic parameters. The results obtained from the simulation was able to effectively model the degradation behavior of the different plastics in this study, thus, predicted the thermal behavior of plastics at different heating rates. However, errors could occur in kinetic parameters obtained when several reactions are occurring simultaneously at the chosen conversion. In addition to this the model is effective in prediction when there no secondary reaction taking place during the degradation process. Aside these shortcomings, DAEM for this study, has proven to be best method in the evaluation of kinetic parameters and all the results obtained using this method was in accordance with literature values.

This goal of this thesis was to convert plastic waste to energy; however, this was not achieved. Notwithstanding from the kinetics of each polymer and the model generated, a good understanding of the pyrolysis process of each polymer was achieved. Further works would be on investigating the kinetics of mixed waste polymer, and how the onset temperature can be reduced. From different literatures it has been observed that the liquid yield from pyrolysis of mixed waste plastic is less than 50%, hence, more studies should be done on understanding the kinetics of mixed waste plastics with either micro-algae, waste agricultural product if co-pyrolysis of these products can increase the liquid yield and quality of hydrocarbon.

Polymers have low conductivity; thus, thermal pyrolysis takes place under high temperature. The use of catalyst could lead to the reaction process to occurring at low temperatures and lower energy use, increased and higher value of yield obtained. Zeolite is the most common catalyst used in plastic pyrolysis, however, this is expensive thus making it not the most economical decision. The use of waste cement as a catalyst in plastic pyrolysis should be investigated because of the possibility of decreasing temperature and prevention of glue formation in the reaction that occurs during thermal pyrolysis.

## Bibliography

- Abbas-Abadi MS, H. M. (2014). Evaluation of Pyrolysis process parameter on polypropylene degradation products. *J Anal Appl Pyrol*, 109:272-7.
- Abnisa F, W. D. (2014). A review on co-pyrolysis of biomass: an optional technique to obtain a high-grade pyrolysis oil. *Energy Conversion Management*, 71–87.
- Aboulkas A, E. h. (2010). Thermal degradation behaviors of polyethylene and polypropylene. Part I: pyrolysis kinetics and mechanisms. *Energy Conversion and Management*, 51:1363–9.
- Achilias, D. S. (2007). Chemical recycling of plastic wastes made from polyethylene (LDPE and HDPE) and polypropylene (PP). *Journal of Hazardous Materials*, 149(3), 536-542. Retrieved from <http://dx.doi.org/10.1016/j.jhazmat.2007.06.076>. PMID:17681427.
- Aguado J, S. D. (2007). Feedstock recycling of polyethylene in a two-step thermo-catalytic reaction system. . *J Anal Appl Pyrol* , 79:415–23.
- Aguado, J. S. (2006). Catalytic upgrading of plastic wastes. pp. 73-110. (& W. In J. Scheirs, Ed.) Hoboken: John Wiley & Sons.
- Ahmad I, I. K. (2013). Catalytic efficiency of some novel nanostructured heterogeneous solid catalysts in pyrolysis of HDPE. . *Polym Degrad Stab* , 98:2512–9.
- Ahmad I, K. M. (2014). Pyrolysis study of polypropylene and polyethylene into premium oil products. *Int J Green Energy* , 12:663–71.
- Alonso, M. Z. (2016, July). A thermogravimetric and kinetic study on devolatilization of woody biomass.
- Arrhenius, S. A. (1889). "Über die Dissociationswärme und den Einfluß der Temperatur auf den Dissociationsgrad der Elektrolyte. *Phys. Chem*, 4: 96–116. doi:10.1515/zpch-1889-0408.
- Arthur, P. (2017). Retrieved from A 5p plastic bag: A short story, highlighting the horrendous plastic pollution in our world seas', and its effect on animals and humans: <https://medium.com/@PaulArthur19602/a-5p-plastic-bag-a-short-story-highlighting-the-horrendous-plastic-pollution-in-our-world-seas-596cc8cc85dd>
- Asensio, R. M. (2009). Analytical characterization of polymers used in conservation and restoration by ATR-FTIR spectroscopy. *Anal. Bioanal. Chem.* 395 (7),, 2081–2096.
- Bagri R, W. P. (2001). Catalytic pyrolysis of polyethylene. *J Anal Appl Pyrol*, 63: 29-41.
- Baines, T. (1993). *New Zealand Energy Information Handbook*. ed. J.T. Baines. Christchurch: Taylor Baines and Associates.
- Barnes, D. K., Galgani, F., Thompson, R. C., & Barlaz, M. (2009, 6 14). Accumulation and fragmentation of plastic debris in global environments. *Philosophical Transactions of the Royal Society B: Biological Sciences*, 364 (1526). doi:10.1098/rstb.2008.0205. PMC 2873009. PMID 19528051
- Beltran, M. M. (1997). Fourier transform infrared spectroscopy applied to the study of PVC decomposition. . *Eur. Polym. J.* 33 (7) , , 1135–1142.

- Blazso, M. (2006). Composition of Liquid Fuels Derived from the Pyrolysis of. p. 315-344. (J. W. J.S.a.W. Kaminsky, Ed.) Budapest , Hungary.
- Buekens, A. (2006). Introduction to feedstock recycling of plastics. In J. Scheirs, & W. Kaminsky (Orgs.), *Feedstock recycling and pyrolysis of waste plastics* . (pp. 3-42) . Hoboken: John Wiley & Sons.
- Cepeliogullar O, P. A. (2013). Utilization of two different types of plastic wastes from daily and industrial life. . (S. S. In: Ozdemir C, Ed.) p. 1–13.
- Chanda, M. (2000). *Advanced polymer chemistry : A problem solving guide*. New York, United State of America.
- Chris Wilcox, E. V. (2005). Threat of plastic pollution to seabirds is global, pervasive, and increasing. Retrieved from <https://doi.org/10.1073/pnas.1502108112>
- Coates, J. (2000). Interpretation of infrared spectra, a practical approach. *Encyclopedia of Analytical Chemistry*, 10815–10837. (R. Meyers, Ed.) Chichester: John Wiley & Sons, Ltd.
- Day, W. E. (2018). Retrieved from Beat Plastics Pollution: <https://www.unenvironment.org/interactive/beat-plastic-pollution/>
- Demirbas A. (2004). Pyrolysis of municipal plastic wastes for recovery of gasoline range hydrocarbon. *J Anal Appl Pyrol*, 72:97–102.
- Donaj PJ, K. W. (2012). Pyrolysis of polyolefins for increasing the yield of monomers' recovery. . *Waste Manage*, 32:840–6.
- Dumitraşa, M. (2014). Non-parametric kinetic analysis of thermogravimetric data for the thermal degradation of poly(tetrafluorethylene). *Acta Chemica Iasi*, 22. 10.2478/achi-2014-0009. .
- Dutton, J. A. (2018). Retrieved from Basic Polymer Structure: <https://www.e-education.psu.edu/matse81/node/2210>
- EAG, L. (2014). *fourier-transform-infrared-spectroscopy-ftir-services*. Retrieved from file:///C:/Users/PC/Downloads/technique-note-fourier-transform-infrared-spectroscopy-ftir-services-m-006216.pdf
- efe-epa. (2018, June 18). Retrieved from Agencia EFE: <https://www.efe.com/efe/english/portada/un-warns-globally-only-9-percent-of-plastic-waste-is-recycled/50000260-3638548#>
- Eriksen, M. L. (2014). Plastic pollution in the world's oceans: more than 5 trillion plastic pieces weighing over 250,000 tons afloat at sea. *PLoS one*, 9(12), e111913.
- Faaij, P. D. (2018). Securing sustainable resource availability of biomass for energy. 26.
- Fakhrhoseini SM, D. M. (2013). Predicting pyrolysis products of PE, PP, and PET using NRTL activity coefficient model. p. 1–5.
- Fakir, Q. (2012). A MODIFIED DISTRIBUTED ACTIVATION ENERGY MODEL FOR THE PYROLYSIS OF SOUTH AFRICAN SOLID FUELS. Retrieved from <https://core.ac.uk/download/pdf/39671187.pdf>
- G, L. (2000). Catalytic degradation of HDPE and PP into liquid fuel in a powder particule fluidized bed. *Polym Degrad Stab*, 70:97-102.



- Geyer, R. J. (2017). Production, use, and fate of all plastics ever made. *Science Advances*, 3(7), e1700782.
- H. Bockhorn, A. H. (1999). *Applied Pyrolysis*.
- H. Polli, L. A. (2009, March). Degradation behavior and kinetic study of ABS polymer. *Journal of Thermal Analysis and Calorimetry*, 95, 131-134. Retrieved from <https://link.springer.com/article/10.1007/s10973-006-7781-1>
- Heikkinen JM, H. J. (2004). Thermogravimetry as a tool to classify waste components to be used for energy generation. *J Anal Appl Pyrol* , 71:883–900.
- Hitachi High Tech. Science Coporation. (1995). Thermal Decomposition Measurement of ABS resin I. Retrieved from [https://www.hitachi-hightech.com/file/global/pdf/products/science/appli/ana/thermal/application\\_TA\\_066e.pdf](https://www.hitachi-hightech.com/file/global/pdf/products/science/appli/ana/thermal/application_TA_066e.pdf)
- Hong S-J, O. S.-P.-O. (1999). A study on the pyrolysis characteristics of poly(vinyl chloride). . *J Korean Inst Chem Eng*, 37:515–21.
- Jeffery D. Peterson, S. V. (2001). Macromol.Chem.Phys.2001,202,775–784 Kinetics of the Thermal and Thermo-Oxidative Degradation of Polystyrene, Polyethylene and Poly(propylene). Center for Thermal Analysis, Department of Chemistry, University of Utah, 315 S. 1400 E., Salt Lake City, UT 84112, USA.
- Jin Woo Park, S. C. (2000). Korean J. Chem. Eng., 17(5), 489-496 (2000)489†To whom correspondence should be addressed. E-mail: khtaik@email.hanyang.ac.kr Kinetic Analysis of Thermal Decomposition of Polymer Using a Dynamic Model. *Korean J. Chem. Eng.*, 17(5), 489-496.
- Jung S-H, C. M.-H.-S.-S. (2010). Pyrolysis of a fraction of waste polypropylene and polyethylene for the recovery of BTX aromatics using a fluidized bed reactor. *Fuel Process Technology*, 91:277–84.
- Kaminsky W, S. B. (1996). Thermal degradation of mixed plastic waste to aromatics and gas. . *Polym Degrad Stab* , 53:189–97.
- KHAWAM, A. (2007). Application of solid state-kinetics to desolvation reactions.
- Kreith, F. (1998). *The CRC handbook of mechanical engineering*. 2nd ed. CRC Press, Inc.;
- Kumar S, S. R. (2011). Recovery of hydrocarbon liquid from waste high density polyethylene by thermal pyrolysis. *Braz J Chem Eng*, 28:659–67.
- Law, K. L. (2017). *Annual review of marine science* 9, 205-229. Retrieved from *Plastics in the marine environment*: <https://www.annualreviews.org/doi/pdf/10.1146/annurev-marine-010816-060409>.
- Lee, K. (2006). Thermal and Catalytic Degradation of Waste HDPE, in *Feedstock Recycling and Pyrolysis of Waste Plastics*. p. 130. Korea: , J. Scheirs and W. Kaminsky, Editors. John Wiley & Sons, Ltd.
- Lettieri, S. A.-S. (2001). Kinetics of Polyethylene Terephthalate (PET) and Polystyrene (PS) Dynamic Pyrolysis. *World Academy of Science, Engineering and Technology/International Journal of Chemical and Molecular Engineering*, 4, No.6,. Retrieved from <https://waset.org/publications/4397/kinetics-of-polyethylene-terephthalate-pet-and-polystyrene-ps-dynamic-pyrolysis>

- Levine, S. a. (2009). Detailed mechanistic modeling of high density polyethylene pyrolysis: Low molecular weight product evolution. *Polymer Degradation and Stability*. 94(5): p. 810-822.
- Liu G, L. Y. (2017). Thermal behavior of vehicle plastic blends contained acrylonitrile-butadiene-styrene (ABS) in pyrolysis using TG-FTIR. doi:doi: 10.1016/j.wasman.2017.01.034.
- Liu Y, Q. J. (1999). Pyrolysis of polystyrene waste in a fluidized-bed reactor to obtain styrene monomer and gasoline fraction. . *Fuel Process Technol*, 63:45–55.
- Madhamshettiwar, D. B. (2014, December). Kinetics and Thermodynamic Studies of Depolymerization of Nylon Waste by Hydrolysis Reaction. (H. Dai, Ed.) *Journal of Applied Chemistry*. Retrieved from <http://dx.doi.org/10.1155/2014/286709>
- Marcilla A, B. M. (2009). Thermal and catalytic pyrolysis of polyethylene over HZSM5 and HUSY zeolites in a batch reactor under dynamic conditions. . *Appl Catal B Environ* , 86:78–86.
- Marcilla, A. B. (2009). Thermal and catalytic pyrolysis of polyethylene over HZSM5 and HUSY zeolites in a batch reactor under dynamic conditions. *Applied Catalysis B: Environmental*, 86(1-2), 78-86. Retrieved from <http://dx.doi.org/10.1016/j.apcatb.2008.07.026>
- Mastral FJ, E. E. (2001). Pyrolysis of high-density polyethylene in a fluidized bed reactor. Influence of the temperature and residence time. . *J Anal Appl Pyrol* , 63:1–15.
- Mastral, J. F. (2007). Theoretical prediction of product distribution of the pyrolysis of high density polyethylene. *Journal of Analytical and Applied Pyrolysis*, 80(2), 427-438. Retrieved from <http://dx.doi.org/10.1016/j.jaap.2006.07.009>
- McMurry, J. (2000). Organic Chemistry. *fifth edition ed. Vol. 5*. Pacific Grove: Brooks/Cole. 172.
- Miandad, R. a.-S. (2019, 02). Catalytic pyrolysis of plastic waste: Moving toward pyrolysis based biorefineries. *Frontiers in Energy Research*, 7, 1-27. doi:10.3389/fenrg.2019.00027
- Miranda R, J. Y. (1998). Vacuum pyrolysis of PVC kinetic study. *Polym Degrad Stab* , 64:127–44.
- Miranda, R. e. (2001). Vacuum pyrolysis of commingled plastics containing PVC II. Product analysis. . *Polymer Degradation and Stability*, 73(1): p. 47- 67.
- Mostafa ME, E.-S. S. (2015). Kinetic parameters determination of biomass pyrolysis fuels using TGA and DTA techniques. *Waste Biomass Valor*, 6:401-415.
- Murata, K. K. (2004). Effect of pressure on thermal degradation of polyethylene. *Journal of Analytical and Applied Pyrolysis*, 71(2): p.569-589.
- Murty, M. e. (1996). Thermal degradation/hydrogenation of commodity plastics and characterization of their liquefaction products. *Fuel Processing Technology*, 49(1-3): p. 75-90.
- Nelson, T. (2017, 12 20). Information System on Plastic Waste Management in Europe. *European Overview*. Retrieved from A Guide by and for Local and Regional Authorities, APME: <http://www.ecvm.org/img/db/ACRRReport.pdf>
- Nishikida, K. C. (2003). Infrared and Raman analysis of polymers. *Handbook of Plastics Analysis*. , 186–316. (J. (. Bonilla, Ed.) New York, USA: Marcel Dekker, Inc, .
- Noda, I. D. (2007). *Group frequency assignments for major infrared bands observed in common synthetic polymers*. (J. (. Mark, Ed.) Physical Properties of Polymers Handbook. Springer Science + Business Media, LLC.

- North, E. J., & Halden, R. U. (2013, 1 1). Plastics and environmental health: The road ahead. *Reviews on Environmental Health*. 28 (1): 1–8. doi:10.1515/reveh-2012-0030. PMC 3791860. PMID 23337043
- Onwudili JA, I. N. (2009). Composition of products from the pyrolysis of polyethylene and polystyrene in a closed batch reactor: effects of temperature and residence time. . *J Anal Appl Pyrol* , 86:293–303.
- Othman N, B. N. (2008). Determination of physical and chemical characteristics of electronic plastic waste (Ep-Waste) resin using proximate and ultimate analysis method. *International conference on construction and building technology*, (pp. p. 169–80).
- Park SS, S. D.-U. ( 2012). Study on pyrolysis characteristics of refuse plastic fuel using lab-scale tube furnace and thermogravimetric analysis reactor. *J Anal Appl Pyrol* , 97:29–38.
- Rafael Balart, D. G.-S.-C.-G. (2019, Feb). Kinetic Analysis of the Thermal Degradation of Recycled Acrylonitrile-Butadiene-Styrene by non-Isothermal Thermogravimetry. *Polymers (Basel)*, v.11(2); PMC6419052. doi: 10.3390/polym11020281
- Richardson, E. (2012). Identification and Classification of Plastics Artefacts. Retrieved from [http://popart-highlights.mnhn.fr/wp-content/uploads/2\\_Identification/5\\_Characterisation\\_of\\_plastics/2\\_6\\_CharacterisationOfPlastics.pdf](http://popart-highlights.mnhn.fr/wp-content/uploads/2_Identification/5_Characterisation_of_plastics/2_6_CharacterisationOfPlastics.pdf)
- Rollinson, R. S. (1999). Kinetics and Mechanisms of the Thermal Degradation of Nylon 6. *Ageing Studies and Lifetime Extension of Materials* , 87-96.
- Ruiz. (2015). Bioenergy potentials for EU and neighbouring countries. *The JRC-EU-TIMES model*.
- S. Venkatachalam, S. G. (2012). Degradation and Recyclability of Poly (Ethylene Terephthalate). Retrieved from [http://cdn.intechopen.com/pdfs/39405/InTech-Degradation\\_and\\_recyclability\\_of\\_poly\\_ethylene\\_terephthalate\\_.pdf](http://cdn.intechopen.com/pdfs/39405/InTech-Degradation_and_recyclability_of_poly_ethylene_terephthalate_.pdf)
- Saha, B. a. (2005). Thermal degradation kinetics of poly (ethylene terephthalate) from waste soft drinks bottles. *Chemical Engineering Journal*, 111(1): p. 39-43.
- Sakata Y, U. M. (1999). Degradation of polyethylene and polypropylene into fuel oil by using solid acid and non-solid acid catalysts. *J Anal Appl Pyrol*, 51:135–55.
- Sakata, Y. U. (1999). Degradation of polyethylene and polypropylene into fuel oil by using solid acid and non-acid catalysts., . *Journal of Analytical and Applied Pyrolysis*, 51(1-2), 135-155.
- Scheirs, J. (2006). Overview of commercial pyrolysis processes for waste plastics. *Feedstock recycling and pyrolysis of waste plastics*, 383-434. (& W. In J. Scheirs, Ed.) Hoboken: John Wiley & Sons.
- Scott, S. D. (2006). An Algorithm for Determining the Kinetics of Devolatilisation of Complex Solid Fuels from Thermogravimetric Experiments. *Chemical Engineering Science*., 61, 2339-2348.
- Seo YH, L. K. (2003). Investigation of catalytic degradation of HDPE by hydrocarbon group type analysis. *J Anal App Pyrol*, 70:383-98.
- Shodhganga. (2012). *Thermal Stability and Degradation Kinetic*. Retrieved from shodhganga@inlibnet: [https://shodhganga.inlibnet.ac.in/bitstream/10603/95342/12/12\\_chapter%205.pdf](https://shodhganga.inlibnet.ac.in/bitstream/10603/95342/12/12_chapter%205.pdf)

- Shodhganga. (2012). Thermal Stability and Degradation Kinetics. Retrieved from Thermal Stability, Degradation Kinetics, Melting, Crystallization and Glass Transition Behaviour: [https://shodhganga.inflibnet.ac.in/bitstream/10603/95342/12/12\\_chapter%205.pdf](https://shodhganga.inflibnet.ac.in/bitstream/10603/95342/12/12_chapter%205.pdf)
- Silvério, F. O.-V. (2008). A pirólise como técnica analítica. *Quimica Nova*. 31(6), 1543-1552. Retrieved from <http://dx.doi.org/10.1590/S0100-40422008000600045>
- Sinfrônio, F. &. (2005). Kinetic of thermal degradation of low-density and high-density polyethylene by non-isothermal thermogravimetry. *Journal of Thermal Analysis and Calorimetry - J THERM ANAL CALORIM*, 79. 393-399.
- Songip, A. e. (1994). Kinetic studies for catalytic cracking of heavy oil from waste plastics over REY zeolite. *Energy and Fuels*. 8(1): p. 131-135.
- Uddin MA, K. K. (1996). Thermal and catalytic degradation of structurally different types of polyethylene into fuel oil. . *Polym Degrad Stab*, 56:37–44.
- Verleye, G. R. (2001). *Easy Identification of Plastics and Rubbers*. Shropshire: Rapra Technology Limited.
- VYAZOVKIN, S., BURNHAM, A., CRIADO, J., MAQUEDA, L., POPESCU, C., & SBIRRAZZUOLI, N. (2011). ICTAC Kinetics Committee recommendations for performing kinetic computations on thermal analysis data., (pp. Acta 520: pp1-19.).
- Wade, L. (1995). The study of chemical reactions. *Organic chemistry. 3rd edition ed.* . Upper Saddle River, New Jersey 07458: Prentice Hall.
- WOJCIECHOWSKI, B. R. (2003). *Experimental Methods in Kinetic Studies*.
- WorldBank. (2019). Retrieved from Trends in Solid Waste Management: [http://datatopics.worldbank.org/what-a-waste/trends\\_in\\_solid\\_waste\\_management.html](http://datatopics.worldbank.org/what-a-waste/trends_in_solid_waste_management.html)
- Wunderlich, B. (2005). *Thermal analysis of Polymeric Materials*. Berlin: Springer.
- Zannikos F, K. S. (2013). Converting biomass and waste plastic to solid fuel briquettes. *J Renew Energy* , 2013:9.

## Annex

Table A-1: Summary of Temperature Ranges for Different Polymer Material

Researcher	Polymer Type	Reactor	Temperature (°C)	Heating Rate (°C/min)	Sweeping Gas	Pressure (MPa)	Residence Time (min)	Crude Oil (wt%)	Gas (wt %)	Residue (wt%)
(Cepeliogullar O, 2013)	PET	Fixed bed	500	10	Nitrogen	-	-	23.1	76.9	-
(Fakhrhoseini SM, 2013)	PET	n/a	500	10	-	-	-	39.89	52.13	8.98
(Ahmad I K. M., 2014)	HDPE	Micro Steel Reactor	300	5–10	Nitrogen	-	-			33.05
			350					80.88		
			400						0.54	
(Kumar S, 2011)	HDPE	Semi-batch	400–550	-	-	-	-	79.08	24.75	-
(Marcilla A, 2009)	HDPE	Batch reactor	550	-	-	-	-	84.7	16.3	-
(Mastral FJ, 2001)	HDPE	Fluidized bed	650	-	-	-	-	68.5	31.5	-
(Miranda R, 1998)	PVC	Batch reactor	225	10	-	0.002	-	0.45		
			520					12.79	19.6	
(Bagri R, 2001)	LDPE	Fixed bed	500	10	Nitrogen	-	20	95		
(Marcilla A, 2009)	LDPE	Batch reactor	550	5	-	-	-	93.1		
(Uddin MA, 1996)	LDPE	Batch reactor	430	-	-	-	-	75.6		
(Aguado J, 2007)	LDPE	Batch reactor	450	-	-	-	-	74.7		
(Onwudili JA, 2009)	LDPE	Batch reactor	425	-	-	0.8 – 4.3	-	89.5	10	0.5
(Ahmad I I. K., 2013)	PP	Micro Steel Reactor	250	-	-	-	-			
			300	-	-	-	-	69.82	1.34	
			400	-	-	-	-		5.7	
(Sakata Y, 1999)	PP	-	380	-	-	-	-	80.1	6.6	13.3
(Fakhrhoseini SM, 2013)	PP	-	500	-	-	-	-	82.12		
(Demirbas A., 2004)	PP	Batch reactor	740	-	-	-	-	48.8	49.6	1.6
(Onwudili JA, 2009)	PS	Batch autoclave	300	10	-	0.3 – 1.6	60			
			425					97	2.5	
			500							
(Liu Y, 1999)	PS	Fluidized bed	450					97.6		
			600					98.7		
			700							
(Kaminsky W, 1996)	0.75 (PE PP), 0.25 (PS)	Fluidized bed	730	-	-	-	-	48.4	-	=-
(Demirbas A., 2004)	PE, PP& PS		730					46.6	35	2.2
(Donaj PJ, 2012)	LDPE, HDPE PP	Bubbling fluidized bed	650	-	-	-	-	48		
			730					44		

## Source Code for DAEM Kinetic Modelling

```
% Kinetic modelling using DAEM for the different plastics
Ea=200 % Initially assumed activation energy
A=1E16 % Initially assumed pre-exponential factor;
R=0.008314 % gas constant kJ/mol.K
B=[(15) (30) (45) ] % Heating rates
%_____

n=100 % Number of reactions
Tr=linspace(300,1000,n) % Temperatures at each reaction
x1 = exp(-((((A*R).(Tr.^2))/(B(1)*Ea)).*(1-(((2*R).*Tr)/Ea))).*exp(-Ea./(R.*Tr))
%X=1-alpha (mass of plastic remaining for the first heating rate)
x2 = exp(-((((A*R).(Tr.^2))/(B(2)*Ea)).*(1-(((2*R).*Tr)/Ea))).*exp(-Ea./(R.*Tr))
%X=1-alpha (mass of plastic remaining for the second heating rate)
x3 = exp(-((((A*R).(Tn.^2))/(B(3)*Ea)).*(1-(((2*R).*Tn)/Ea))).*exp(-Ea./(R.*Tr))
%X=1-alpha (mass of plastic remaining for the third heating rate)
%_____

%plot of the mass remaining as a function of temperature
plot(Tr,x1,'m',Tr,x2,'g',Tr,x3,'r')
title(' Simulated thermogravimetric analysis','FontWeight','bold')
xlabel('Temperature(K)');ylabel('Weight % remaining')
% The DAEM model for the simulated profile obtained using solver
U=linspace(0.9999,0.0001,n); % Initially assumed conversions for100 reactions
% Calculate the temperatures corresponding to the assumed number of reactions
%This will be done by solving between the results obtained from solver and the DAEM curve
for i=1:n
    T1(i)=fzero(@(T)(U(i)-exp(-((((A*R).(T.^2))/(B(1)*Ea)).*(1-(((2*R).*T)/Ea))).*exp(- Ea./(R.*T)))),500)
    T2(i)=fzero(@(T)(U(i)-exp(-((((A*R).(T.^2))/(B(2)*Ea)).*(1-(((2*R).*T)/Ea))).*exp(- Ea./(R.*T)))),500)
    T3(i)=fzero(@(T)(U(i)-exp(-((((A*R).(T.^2))/(B(3)*Ea)).*(1-(((2*R).*T)/Ea))).*exp(- Ea./(R.*T)))),500)
end;
% Parameters for the Simulated reactions
```

```

T0=400; % Initial temperature of the plastic
E0=200; % Initial assumed activation energy

% %
_____

for j=1:n
    Ti1=T1(j)
    Ti2=T2(j)

    % Activation energy

    E(j)=fzero(@(E)((1/B(1))*(T0*exp(-E/(R*T0)))-(E/R)*expint(E/(R*T0))-Ti1*exp(-
    E/(R*Ti1)))+(E/R)*expint(E/(R*Ti1))))...

        -((1/B(2))*(T0*exp(-E/(R*T0)))-(E/R)*expint(E/(R*T0))-Ti2*exp(-
    E/(R*Ti2)))+(E/R)*expint(E/(R*Ti2))))),E0)

    %Activation energy

    %Pre-exponential Factor

    A(j)=-B(1)/(T0*exp(-E(j)/(R*T0))-(E(j)/R)*expint(E(j)/(R*T0))-Ti2*exp(-
    E(j)/(R*Ti2)))+(E(j)/R)*expint(E(j)/(R*Ti2)))

end

E % Activation energy

A %Pre-exponential factor

%writematrix([A,Tr],'values1.xls')

clc

clear all

o=1.000;%order of reaction

R=0.008314 % gas constant kJ/mol.k

A=6E16;% Pre-exponential Factor

Em=220;%Mean activation energy, kJ/mol

d=15;% Standard deviation, kJ/mol

Emin=50;%Minimum activation energy

Emax=350;%Maximum activation energy

B=[15 30 45];%heating rates

```

```

Tg=linspace(300,700,n);%temperatures at each reaction

for i=1:length(B)
for j=1:length(Tg)

Tr=Tg(j);

W(i,j)=quad(@(E)(((1-(1-o)*(Ac*R*Tr^2./(B(i)*E)).*exp(-E/(R*Tr)).*(1-(2*R*Tr./E))).^(1/(1- o))).*...
((1/(d*sqrt(2*pi))).*exp(-(E-Em).^2/(2*d^2))),Emin,Emax);

%weight% remaining

end

W;

%-----

n=100;%assumed number of reactions for the model

X=linspace(0.99,0.001,n);% assumed conversions for the model

Ta1=(interp1q(flipud(W(1,:)),flipud(Tg'),flipud(X')));

Ta1=(flipud(Ta1));%Temperature for first heating rate

Tb1=(interp1q(flipud(W(2,:)),flipud(Tg'),flipud(X')));

Tb1=(flipud(Tb1));%Temperature for second heating rate

%Check Temperature=[X' Ta1' Tb1']%Confirmation of temperature data accuracy %-----
-----

% Kinetic modelling using DAEM for the different plastics

T0=379;% Initial temperature of the plastic

E0=200;% % Initial assumed activation energy

xi=1-exp(-1);%conversion needed to evaluate pre exponential factor

for j=1:n

Ti1=Ta1(j);

Ti2=Tb1(j);

E(j)=fzero(@(E)((R*Ti1^2/(B(1)*E))*exp(-E/(R*Ti1))*(1-(2*R*Ti1/E)))-...
((R*Ti2^2/(B(2)*E))*exp(-E/(R*Ti2))*(1-(2*R*Ti2/E))),E0);

%Activation energy

A(j)=(1/(1-o))*(1-xi^(1-o))*(B(1)*E(j))/(R*Ti1^2*exp(-E(j)/(R*Ti1))*(1- (2*R*Ti1/E(j))));

end

```



```

E;%
A;%
%Determining the mass initial mass fraction
n=100;%assumed number of reactions for the model
T=linspace(300,700,n); % temperatures required to evaluate the model
chm1=zeros(n+1);% generation of zero matrix
chm1(:,end)=1; % 1 's in the end of each row
chm1(1,:)=1; % 1's in column this corresponds to 100 % mass remaining
for k=1:n;
for z=1:n;
%chm1(k+1,z)=exp((-A(z)/B(1)).*quad(@(T)exp(-E(z)./(R*T)),T0,T1(k)));
end
end
chm1;
M1=[1 X]'; % matrix of remaining mass
f1=lsqnonneg(chm1,M1)
%_____

% % Matrix for the first heating rate
chm2=zeros(n+1);
chm2(:,end)=1;
chm2(1,:)=1;
for k=1:n;
for z=1:n;% for the columns chm2(k+1,z)=exp((-A(z)/B(1))*quad(@(T)exp(-E(z)./(R*T)),T0,T(k)));
end
end
chm2;
S2=chm2*f1;
Tg2=[T0 T]';
plot(Tg2,S2,'.b')
%_____

```